Copy No. 142
RM No. L8E12

NACA RM No. L8E12

NACA

RESEARCH MEMORANDUM

LONGITUDINAL STABILITY CHARACTERISTICS OF A 42° SWEPTBACK WING AND TAIL COMBINATION AT A REYNOLDS NUMBER OF 6.8×10^6

By

Stanley H. Spooner and Albert P. Martina

Langley Aeronautical Laboratory
Langley Field, Va.

NATIONAL ADVISORY COMMITTEE FOR AERONAUTICS

WASHINGTON

July 22, 1948

NATIONAL ADVISORY COMMITTEE FOR AERONAUTICS

RESEARCH MEMORANDUM

LONGITUDINAL STABILITY CHARACTERISTICS OF A 42° SWEPTBACK WING AND TAIL COMBINATION AT A REYNOLDS NUMBER OF 6.8×10^6

By Stanley H. Spooner and Albert P. Martina

SUMMARY

A wind-tunnel investigation has been conducted at a Reynolds number of 6.8×10^6 and at a Mach number of 0.14 to determine the longitudinal stability characteristics of an airplane configuration with a 42° sweptback wing and horizontal tail. The wing had an aspect ratio of 4.01, a taper ratio of 0.625, and NACA 64_1-112 airfoil sections. The effects of the vertical positions of the fuselage and horizontal tail with respect to the wing were determined for several combinations of high-lift and stall-control devices. The characteristics in the presence of a simulated ground were also determined.

For lift coefficients at which wing stalling occurred, the tail positions on or below the wing-chord plane extended provided the most stability; whereas for lift coefficients below the stall, the greatest stability was obtained with the highest tail positions.

The tail did not appreciably alter the direction of the final break in the pitching-moment curve of the model in the stalling range, except that in most cases when the tail was located near or below the wing-chord plane extended, the tail caused an unstable break to become stable. Tail positions at moderate heights, approximately 0.15 semispan to 0.25 semispan above the chord plane extended, often resulted in the least desirable pitching-moment characteristics of the vertical positions investigated.

The effect of the leading-edge stall-control devices was to delay or eliminate the tip stall and thus cause the final break of the pitching-moment curve to be in a stable direction. The application of fences on the upper surface of the wing tended to eliminate the small region of instability preceding maximum lift.

The effect of the tail on the pitching-moment characteristics was not altered appreciably by the relative wing-fuselage height.

The tests of the model in the presence of a simulated ground (ground board) showed a reduction in the rate of change of effective

downwash angle with angle of attack for angles of attack up to those at which wing stalling occurred. The neutral points were shifted rearward with increasing angle of attack. In the range in which wing stalling occurred, no appreciable ground effect was discernible. The effects of the tail vertical position and the leading-edge flaps in the presence of the ground board were, in general, similar to those without the ground board.

INTRODUCTION

Unpublished results of previous investigations of a 42° sweptback wing-fuselage combination have shown the longitudinal stability in the region of maximum lift to be dependent upon the stalling pattern of the wing, with wing-tip stall giving an unstable break in the pitching-moment curve. The basic wing-fuselage combination exhibited unstable characteristics in the maximum-lift region which were, however, generally moderated or relieved by the use of adequate stall-control devices. Since the downwash field behind the wing would be affected appreciably by these devices, it was deemed necessary to determine the characteristics of the model with a sweptback horizontal tail located at several vertical positions.

The investigation reported herein shows the effects on the longitudinal stability of vertical position of the wing with respect to the fuselage and of the tail to the wing for numerous flap configurations. The flap configurations include partial-span split flaps in conjunction with leading-edge flaps, leading-edge slats, and fences on the upper surface of the wing. The influence of a ground board on the longitudinal stability characteristics of the model is also shown for a few configurations. The investigation was conducted at a Reynolds number of approximately 6.8×10^6 and at a Mach number of about 0.14 in the Langley 19-foot pressure tunnel.

SYMBOLS

C_L	lift coefficient (L/qS)
C_m	pitching-moment coefficient $(M/qS\bar{c})$
L	lift, pounds
M	pitching moment about quarter-chord point of mean aerodynamic chord, foot-pounds
q	free-stream dynamic pressure $\left(\frac{1}{2}\rho V^2\right)$

S wing area, 32.24 feet^2

$\bar{c}$ wing mean aerodynamic chord (M.A.C.) measured parallel to plane of symmetry, 2.892 feet $\left(\frac{2}{S}\int_0^{b/2} c^2\,dy\right)$

ρ mass density of air, slugs per cubic foot

V velocity, feet per second

c local wing chord measured parallel to plane of symmetry, feet

b wing span measured normal to plane of symmetry, 11.375 feet

y spanwise distance, feet

α angle of attack of wing chord, degrees

ϵ effective downwash angle, degrees

q_t/q ratio of effective dynamic pressure at the tail to free-stream dynamic pressure

$d\epsilon/d\alpha$ rate of change of effective downwash angle with angle of attack

i_t angle of incidence of horizontal tail with respect to wing chord, degrees

MODEL

The principal dimensions of the model are shown in figure 1. The wing had an angle of sweepback of 42.05° at the leading edge and NACA 64_1-112 airfoil sections perpendicular to the 0.273-chord line. The 0.273-chord line corresponds to the 0.25-chord line before the wing panels were swept back. The wing had an aspect ratio of 4.01, a taper ratio of 0.625, and no twist or dihedral. The area of the horizontal tail was 16 percent of the area of the wing, and the horizontal tail was geometrically similar to the wing except that the tail had NACA 0012-64 airfoil sections parallel to the plane of symmetry. Measured perpendicular to the 0.273-chord line, the maximum thickness of the tail amounted to approximately 15 percent of the local chord of the tail. An airfoil of 15-percent thickness was dictated by installation considerations, but it is believed that a tail with somewhat thinner sections would not appreciably alter the stability characteristics of the model.

The fuselage had a fineness ratio of 10.2:1 and was circular in cross section. The maximum diameter, which was constant over that section of the fuselage intersected by the wing, was 12.3 percent of the wing span. The 0.273-chord point of the wing root was located 37.5 percent of the maximum fuselage diameter above and below the fuselage center line for the high-wing and low-wing configurations and on the center line for the midwing configuration. In each of the three positions tested, the wing-chord plane had a positive angle of incidence of 2° with respect to the fuselage center line. No fillets were used at the wing-fuselage juncture.

The relative locations of the tail and the wing-chord plane extended are shown in figure 2. The tail length used was equal to $2\bar{c}$ measured between the quarter-chord points of the wing and tail mean aerodynamic chords parallel to the wing-chord plane. The tail height was varied by using a tail post of adjustable length. The incidence of the tail was measured with respect to the wing-chord plane and was changed by rotating the tail about a line normal to the plane of symmetry and through the quarter-chord point of its mean aerodynamic chord.

The several high-lift and stall-control devices used on the model are shown in figure 3. The split flaps had a chord of 0.184c measured parallel to the plane of symmetry and were deflected 60° measured between the wing lower surface and the flap in a plane perpendicular to the hinge line; they extended from 50 percent of the semispan inboard to 12.3 percent of the semispan.

The spans of the leading-edge flaps investigated were $0.725\frac{b}{2}$ and $0.575\frac{b}{2}$. The outboard ends of these flaps were located at 97.5 percent of the semispan (beginning of rounded tip). The leading-edge flaps were of constant chord and amounted to 14.3 percent of the local chord at the outboard end. The flaps were deflected 50° and were measured in the manner shown in figure 3.

The chord of the leading-edge slat was 22.1 percent of the local wing chord measured parallel to the plane of symmetry. The slat span was $0.575\frac{b}{2}$ with the outboard end located at $0.975\frac{b}{2}$. The upper surface and the leading edge of the slat had the same contour as the airfoil of the wing and the wing was cut out so that the slat in the retracted position formed the wing leading edge. The location of the slat in the extended position is shown in figure 3.

The upper-surface fences were mounted normal to the wing surface and parallel to the plane of symmetry. They projected 0.6 of the maximum thickness of the airfoil section above the wing surface. When

used in conjunction with the leading-edge flap or the slat, the fences extended from the wing trailing edge to the 0.05-chord line and to the 0.22-chord line, respectively. In a spanwise direction the fences were located $0.05\frac{b}{2}$ outboard of the inboard end of the leading-edge flaps or slat.

The model was constructed of steel and mahogany. The flaps were of sheet steel whereas the slat was made of machined aluminum. The model was lacquered and sanded to obtain an aerodynamically smooth surface. The model mounted for testing in the Langley 19-foot pressure tunnel is presented as figure 4.

TESTS

The tests were made in the Langley 19-foot pressure tunnel with the air in the tunnel compressed to approximately $2\frac{1}{3}$ atmospheres. Measurements of the lift and pitching moment for each model configuration were made through an angle-of-attack range from near zero lift to beyond maximum lift except as limited by the mechanical setup. The tests were conducted at a dynamic pressure of approximately 75 pounds per square foot which corresponds to a Mach number of 0.14 and a Reynolds number of 6.8×10^6 based on the wing mean aerodynamic chord.

The ground-effect tests were made through the use of a ground board spanning the test section of the tunnel and extending several chords ahead of and behind the model. The boundary layer over the ground board was kept thin by means of spanwise suction slots located on the ground board in the vicinity of the model, and no flow separation was encountered. The quarter-chord point of the wing mean aerodynamic chord was maintained at a constant height of $0.92\bar{c}$ above the ground plane for all configurations. The model and ground-board installations are presented as figure 5.

The tests of the isolated tail were made by using the setup shown in figure 6 and were conducted at a Reynolds number of approximately 2.7×10^6 which corresponded to a Reynolds number of 6.8×10^6 based on the wing mean aerodynamic chord.

RESULTS AND DISCUSSION

All force and moment data have been reduced to standard nondimensional coefficients. Corrections have been determined and applied to the force and moment data obtained from the tests to account

for the tare and interference effects of the model support system. Stream-angle and jet-boundary corrections have been applied to the angle of attack for the tests without the ground board. Jet-boundary corrections have also been applied to the pitching-moment data. Calculations indicated that the jet-boundary corrections applicable to the data from tests using the ground board were negligible and, therefore, such corrections were not applied. It was not feasible to determine tares for the isolated-tail data.

The results of the tests are given in figures 7 to 9. The variation of angle of attack with pitching-moment coefficient, lift coefficient, effective downwash angle, and dynamic-pressure ratio at the tail are shown in figure 7 for the various configurations. Data for only one of the two tail incidences used at each tail height have been presented. The dynamic-pressure ratio q_t/q was determined from the ratio of the tail effectiveness obtained from the tail-on tests to that calculated from the isolated-tail test. The effectiveness dC_m/di_t calculated from the isolated-tail test was -0.0166. It should be pointed out that by using the isolated tail data to compute dC_m/di_t no account was made for a reduction in tail efficiency due to the tail operating in the presence of the fuselage. The downwash values were computed from the pitching-moment data for the tests of the model with and without the horizontal tail. Values of $d\epsilon/d\alpha$ for the linear part of the lift curves are presented in table I. The various model configurations and their pitching-moment curves are illustrated in table II.

The neutral points calculated for several configurations are shown in figure 8. The isolated-tail lift curve is shown in figure 9.

Effects of Tail Vertical Position

Linear lift range.- As may be seen from figures 7(a) to 7(o) and as shown in table I for the range of lift coefficients up to those at which separation occurs on the wing, the lowest values of $d\epsilon/d\alpha$ were generally obtained with the highest of the tail positions tested. At low lift coefficients the tail positions in the vicinity of the chord plane extended usually resulted in larger values of $d\epsilon/d\alpha$ than did the tail positions at moderate heights $\left(0.25\frac{b}{2}\right)$ above the chord plane extended. At higher lift coefficients, however, the values of $d\epsilon/d\alpha$ were larger for tail positions at moderate heights above the chord plane extended than for those in the vicinity of the chord plane extended. It is of interest to note that in the linear lift range the smallest values of downwash were obtained with the horizontal tail located near the wing-chord plane extended. (For example, see fig. 7(a).) Much of this effect is probably due to fuselage interference.

Values of the dynamic-pressure ratio at the tail q_t/q of about unity were obtained for the high tail positions whereas values up to

20 percent less were obtained for the low tail positions. As might be expected from the small values of $d\epsilon/d\alpha$ and the large values of q_t/q, greater stability was obtained with the high tail positions for the lift range below the stall as shown by the neutral point curves of figure 8.

Nonlinear lift range.- In the angle-of-attack range where flow separation occurred, the largest values of $d\epsilon/d\alpha$ (approaching 2.0) were obtained for tail positions above the wing-chord plane extended. The low tail positions usually resulted in the smallest values of $d\epsilon/d\alpha$ which approached zero or even became negative. The small values of $d\epsilon/d\alpha$ were probably the result of the tail operating in or below the wing wake. The magnitude of $d\epsilon/d\alpha$ in the region of maximum lift was also dependent upon the wing stalling pattern and resultant load distribution of the particular flap configuration.

In the stalling range, q_t/q showed no consistent changes with the vertical location of the horizontal tail.

The effects of the tail vertical position on the pitching-moment characteristics in the region of maximum lift are summarized in table II. The addition of the tail in the vicinity of the wing-chord plane extended improved the stability and generally caused stable breaks in the pitching-moment curves even though the wing-fuselage combination was unstable. Similar effects were observed in reference 1. For positions at moderate heights, approximately $0.15\frac{b}{2}$ to $0.25\frac{b}{2}$ above the chord plane extended, the tail was ineffective in influencing tail-off stability at high angles of attack. For configurations with leading-edge flaps or slats the angle of attack at which the tail became ineffective increased with tail height. The stability of these configurations in the stalling range was then critically dependent upon the degree of stability of the wing-fuselage combination and the tail height. For configurations without leading-edge devices the tail produced no favorable effects for tail heights above the wing-chord plane extended. In a few cases (for example, see fig. 7(o)) tail locations at moderate heights $\left(0.25\frac{b}{2}\right)$ above the chord plane extended resulted in the least desirable pitching-moment characteristics of any of the vertical positions investigated. In this particular instance, the tail is probably operating in the wake of the wing as indicated by the rapid decrease in q_t/q. Another contributing factor, although not isolated here, may be separation at the wing-fuselage juncture.

It should be noted that the fuselage used in this investigation was not necessarily an optimum design and that a fuselage with a

less rapid contraction rate on the rear portion, together with proper filleting at the wing juncture, might alter the stability characteristics for tail positions close to the fuselage.

Effect of High-Lift and Stall-Control Devices

In general, for angles of attack below those at which air-flow separation begins, the addition of the high-lift and stall-control devices did not appreciably alter the values of $d\epsilon/d\alpha$ from those obtained with the unflapped wing. At angles of attack at which air-flow separation occurred, the high-lift and stall-control devices generally gave lower values of $d\epsilon/d\alpha$ than those of the unflapped wing. This effect may be explained by the inward movement of the spanwise center of pressure which occurred when the tip region of the unflapped wing stalled; whereas for the flapped configurations, the spanwise center of pressure was shifted outward by the area of separated flow near the wing root. Similarly, the larger span leading-edge flap tested gave the lower values of $d\epsilon/d\alpha$.

The upper-surface fences tested on the wing in conjunction with either the leading-edge flaps or slats produced little change in the downwash characteristics except at a small range of angle of attack in the vicinity of maximum lift where the fences tended to restrict the regions of separated flow to areas inboard of the fences, which separated regions caused the downwash to increase less rapidly.

The addition of the leading-edge flaps or slats and trailing-edge split flaps to the wing resulted in a forward movement of the neutral point of up to 5 percent for lift coefficients below the stall, as shown in figure 8. As the span of the leading-edge flaps was increased toward the wing root, furthermore, the neutral point was moved forward because of the increased wing area ahead of the quarter chord of the wing mean aerodynamic chord.

Because of the large values of $d\epsilon/d\alpha$ in the angle-of-attack range immediately preceding maximum lift, instability was obtained for tail positions above the chord plane extended except for the highest position. (See figs. 7(d) to 7(f).) This undesirable condition was eliminated in most cases by the use of the upper-surface fences (figs. 7(g) and 7(h)). The final break in the pitching-moment curve of the model with stall-control devices was not appreciably altered by the horizontal tail.

For the model investigated, a low-wing configuration with partial-span split flaps, upper-surface fences, and leading-edge flaps spanning the outer 65 to 70 percent of the semispan might be a good compromise between the higher maximum lift characteristics of the $0.725\frac{b}{2}$ flaps

and the more stable pitching-moment characteristics of the $0.575\frac{b}{2}$ flaps. With this configuration the tail might be located in any vertical position except above and adjacent to the fuselage.

Effects of Wing-Fuselage Vertical Position

Linear lift range.- The relative position of the wing and fuselage appears to be of secondary importance as regards the effect of the tail on the longitudinal stability. An indication of the effects may be seen by comparing figures 7(a) and 7(c) for the flaps-off condition and figures 7(d), 7(f), 7(i), and 7(k) for the wing with flaps. For the same tail position, $0.25\frac{b}{2}$ above the wing-chord plane extended, the values of $d\epsilon/d\alpha$ (table I) were approximately equal for either the high-wing or low-wing configuration in the angle-of-attack range up to the stall. The values of the downwash angles at given angles of attack up to the stall were about 1° less for the high-wing configuration than for the low-wing configuration with flaps off, whereas no noticeable difference was apparent for the flapped wing.

As may be seen from figure 8, the effect of raising the wing from the low to the high position was to bring about a forward movement of the neutral point, which averaged 2 percent of the mean aerodynamic chord, for this particular tail position $\left(0.25\frac{b}{2}\right.$ above the chord plane extended$\left.\right)$.

Nonlinear lift range.- For the flapped configurations the values of $d\epsilon/d\alpha$ for tail positions $0.25\frac{b}{2}$ above the chord plane extended were generally greater for the high-wing configurations than for the low-wing configurations. Although the pitching-moment characteristics of the basic configurations were somewhat affected by the relative vertical position of the wing and fuselage, the addition of the tail did not appreciably alter these effects.

Ground Effect

A comparison of the results for the ground board (see figs. 7(p) to 7(r) and table I) with the results of similar model configurations for the ground board out indicates that the ground effect reduced $d\epsilon/d\alpha$ for angles of attack up to maximum lift as expected. Figure 8 indicates that the neutral points are shifted rearward with an increase in lift coefficient. This change is probably due to a progressively increasing slope of the tail lift curve as the tail approaches the ground with increase in angle of attack.

In the stalling region there was generally no large change in the stability due to the ground board.

The effects of the tail height and the leading-edge flaps in the presence of the ground board were, in general, similar to those without the ground board.

CONCLUSIONS

From the results of wind-tunnel tests of a 42° sweptback wing-fuselage combination with NACA 64_1-112 airfoil sections and a sweptback horizontal tail, the following conclusions may be drawn:

1. For lift coefficients at which wing stalling occurred, the tail positions on or below the wing-chord plane extended provided the most stability; whereas for lift coefficients below the stall, the greatest stability was obtained with the highest tail positions.

2. The horizontal tail used in the present tests did not appreciably alter the direction of the final break in the pitching-moment curve of the model in the stalling range except when it was located near or below the wing-chord plane extended. In most cases the tail located near the chord plane extended caused an unstable break in the pitching-moment curve to become stable. Tail positions at moderate heights, approximately 0.15 semispan to 0.25 semispan above the chord plane extended, often resulted in the least desirable pitching-moment characteristics of the vertical positions investigated.

3. The effect of the leading-edge stall-control devices was to delay or eliminate the tip stall and thus cause the final break of the pitching-moment curve to be in a stable direction. The application of fences on the upper surface of the wing tended to eliminate the small region of instability preceding maximum lift.

4. The effect of the tail on the pitching-moment characteristics was not altered appreciably by the relative wing-fuselage height.

5. The ground board caused a reduction in the rate of change of effective downwash angle with angle of attack for angles of attack up to those at which wing stalling occurred. The neutral points were shifted rearward with increasing angle of attack or lift coefficient. In the range in which wing stalling occurred, no appreciable ground

effect was discernible. The effects of the tail height and the leading-edge flaps in the presence of the ground board were, in general, similar to those without the ground board.

Langley Memorial Aeronautical Laboratory
National Advisory Committee for Aeronautics
Langley Field, Va.

REFERENCE

1. Purser, Paul E., Spearman, M. Leroy, and Bates, William R.: Preliminary Investigation at Low Speed of Downwash Characteristics of Small-Scale Sweptback Wings. NACA TN No. 1378, 1947.

TABLE I.- MEASURED VALUES OF $d\epsilon/d\alpha$ IN THE LINEAR LIFT RANGE

Configuration			Tail height (percent b/2)	$d\epsilon/d\alpha$	Reference figure
Flap	Ground board	Wing position			
Off	Out	Low	50.9	0.38 decreasing to 0.25	7(a)
			25.4	0.45	
			3.1	0.54 decreasing to 0.19	
		Mid	41.7	0.41	7(b)
			16.2	0.47 increasing to 0.56	
			-6.1	0.46	
		High	25.4	0.44	7(c)
			-14.6	0.41	
0.575 $\frac{b}{2}$-span leading-edge flaps and split flaps	Out	Low	50.9	0.33	7(d)
			25.4	0.44	
			3.1	0.36	
		Mid	41.7	0.42	7(e)
			16.2	0.36	
			-6.1	0.41	
		High	25.4	0.45	7(f)
			-14.6	0.51 decreasing to 0.30	
0.575 $\frac{b}{2}$-span leading-edge flaps, split flaps, and fences	Out	Low	50.9	0.35	7(g)
			25.4	0.43	
			3.1	0.44	
		Mid	41.7	0.39	7(h)
			16.2	0.44	
0.725 $\frac{b}{2}$-span leading-edge flaps, and split flaps,	Out	Low	50.9	0.34	7(i)
			25.4	0.44	
			3.1	0.46 decreasing to 0.25	
		Mid	41.7	0.39	7(j)
			16.2	0.41	
			-6.1	0.43	
		High	25.4	0.43	7(k)
			-14.6	0.54 decreasing to 0.40	
0.725 $\frac{b}{2}$-span leading-edge flaps, split flaps, and fences	Out	Low	25.4	0.43	7(l)
			3.1	0.46 decreasing to 0.34	
		Mid	41.7	0.43	7(m)
			16.2	0.46	
0.575 $\frac{b}{2}$-span slat and split flaps	Out	Low	50.9	0.35	7(n)
			25.4	0.40	
			3.1	0.45 decreasing to 0.23	
0.575 $\frac{b}{2}$-span slat, split flaps, and fences	Out	Low	50.9	0.35 increasing to 0.40	7(o)
			25.4	0.41	
			3.1	0.48 decreasing to 0.31	
Off	In	Low	50.9	0.22	7(p)
			25.4	0.30	
			3.1	0.32 decreasing to 0	
0.575 $\frac{b}{2}$-span leading-edge flaps and split flaps	In	Low	50.9	0.21	7(q)
			25.4	0.21	
			3.1	0.15 decreasing to 0	
0.725 $\frac{b}{2}$-span leading-edge flaps and split flaps	In	Low	50.9	0.22 decreasing to 0.08	7(r)
			25.4	0.20 decreasing to 0.08	
			3.1	0.20 decreasing to -0.10	

TABLE II.- SUMMARY OF PITCHING-MOMENT CHARACTERISTICS OF 42° SWEPTBACK WING FUSELAGE COMBINATION WITH SWEPTBACK HORIZONTAL TAIL

Configuration		Tail height (percent b/2 above chord plane extended)	C_m characteristics	
Flap	Wing		Ground board in	Ground board out
Off	Low	Tail off	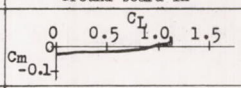	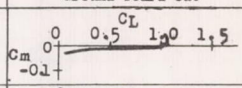
		50.9	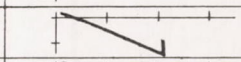	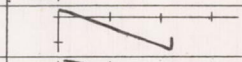
		25.4	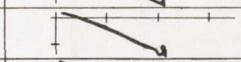	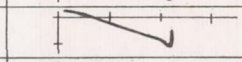
		3.1	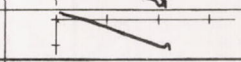	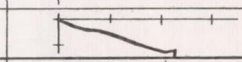
	Mid	Tail off		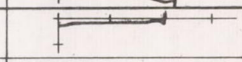
		41.7		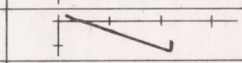
		16.2		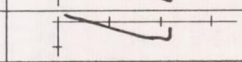
		-6.1		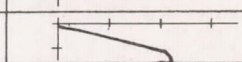
	High	Tail off		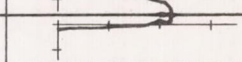
		25.4		
		-14.6		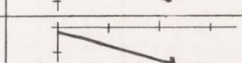
$0.575\frac{b}{2}$ - span leading-edge flaps and split flaps	Low	Tail off	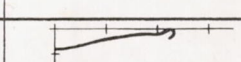	
		50.9		
		25.4		
		3.1	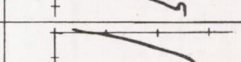	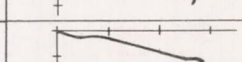
	Mid	Tail off		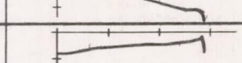
		41.7		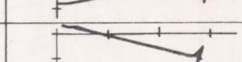
		16.2		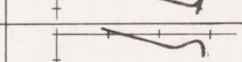
		-6.1		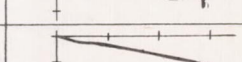
	High	Tail off		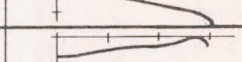
		25.4		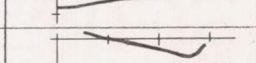
		-14.6		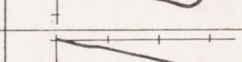
$0.575\frac{b}{2}$ - span leading-edge flaps, split flaps, and fences	Low	Tail off		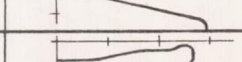
		50.9		
		25.4		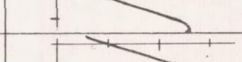
		3.1		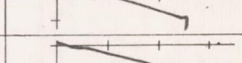
	Mid	Tail off		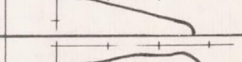
		41.7		
		16.2		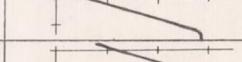

TABLE II.- SUMMARY OF PITCHING-MOMENT CHARACTERISTICS OF 42° SWEPTBACK WING FUSELAGE COMBINATION WITH SWEPTBACK HORIZONTAL TAIL - Concluded

Configuration		Tail height (percent b/2 above chord plane extended)	C_m characteristics	
Flap	Wing		Ground board in	Ground board out
$0.725\frac{b}{2}$ - span leading-edge flaps and split flaps	Low	Tail off	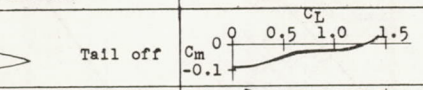	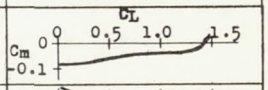
		50.9	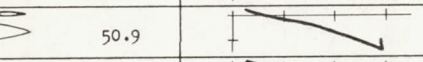	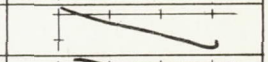
		25.4	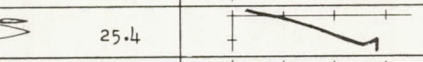	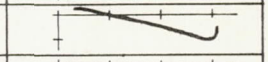
		3.1	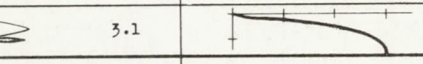	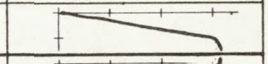
	Mid	Tail off		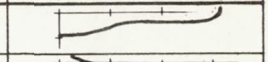
		41.7		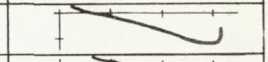
		16.2		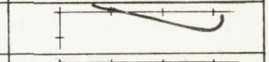
		-6.1		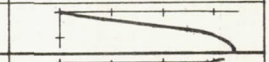
	High	Tail off		
		25.4		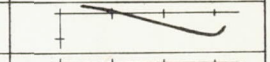
		-14.6		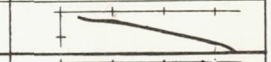
$0.725\frac{b}{2}$ - span leading-edge flaps, split flaps, and fences	Low	Tail off		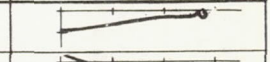
		25.4		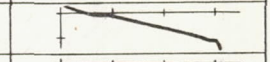
		3.1		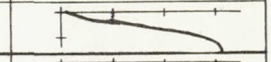
	Mid	Tail off		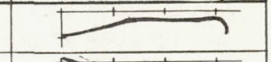
		41.7		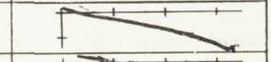
		16.2		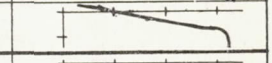
$0.575\frac{b}{2}$ - span leading-edge slat and split flaps	Low	Tail off		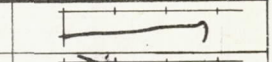
		50.9		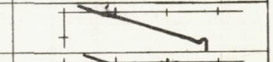
		25.4		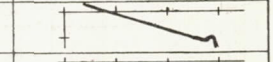
		3.1		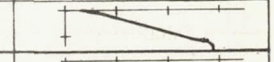
$0.575\frac{b}{2}$ - span leading-edge slat, split flaps, and fences	Low	Tail off		
		50.9		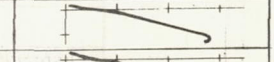
		25.4		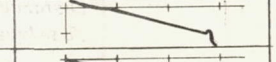
		3.1		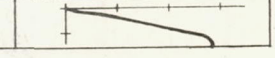

NACA

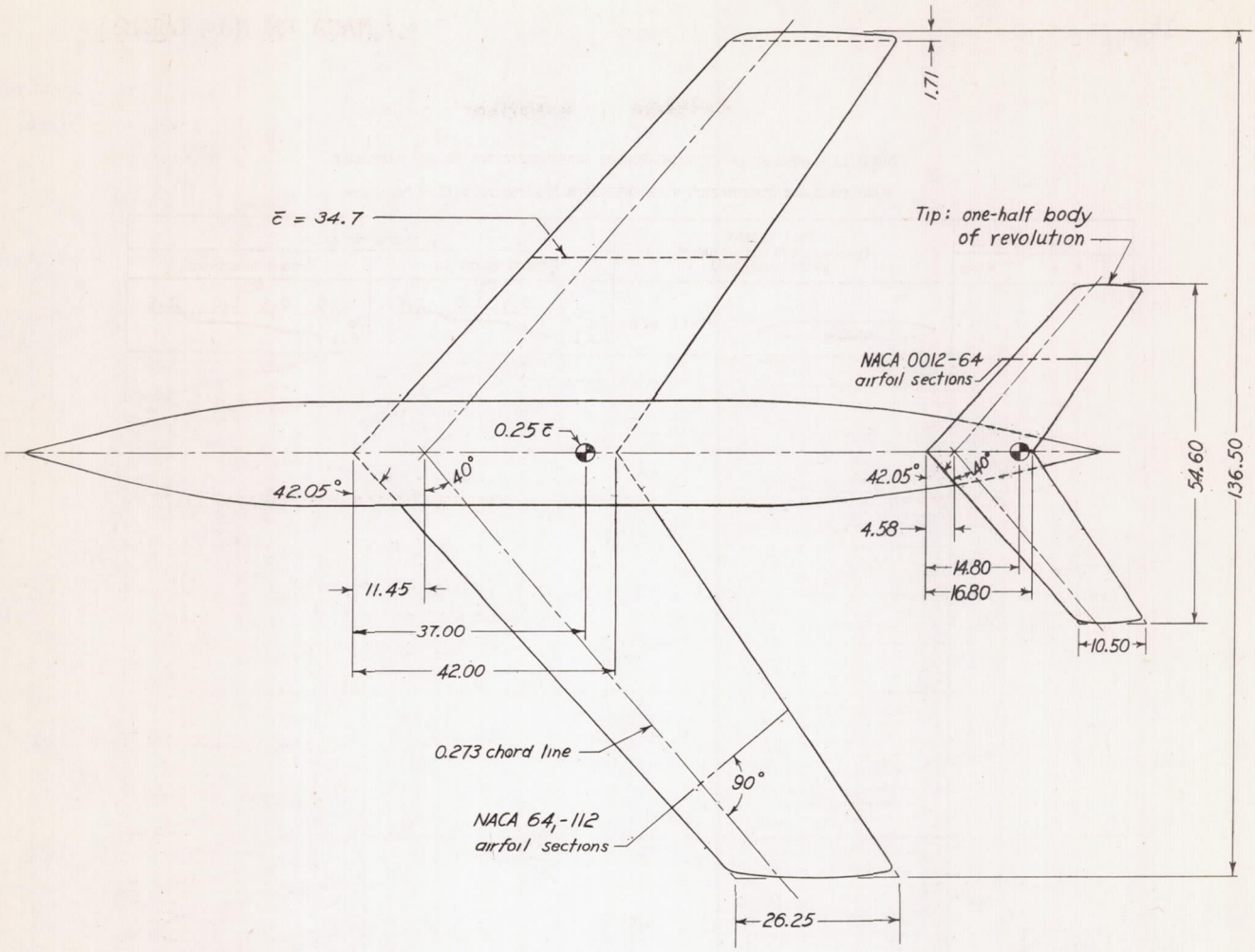

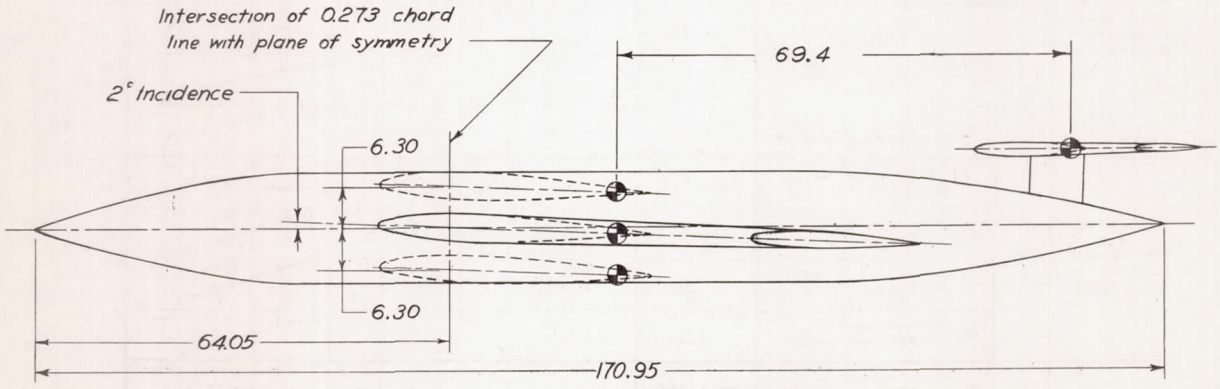

FUSELAGE ORDINATES

Distance behind fuselage nose	Fuselage diameter	Distance behind fuselage nose	Fuselage diameter
0	0.20	112.00	16.80
18.00	9.84	122.00	16.32
22.05	11.80	132.00	14.90
27.39	13.80	142.00	12.52
34.56	15.60	151.20	9.46
42.35	16.60	162.00	4.78
48.00	16.80	170.95	0

Figure 1.- Geometry of model. Aspect ratio, 4.01; taper ratio, 0.625. (All dimensions are in inches.)

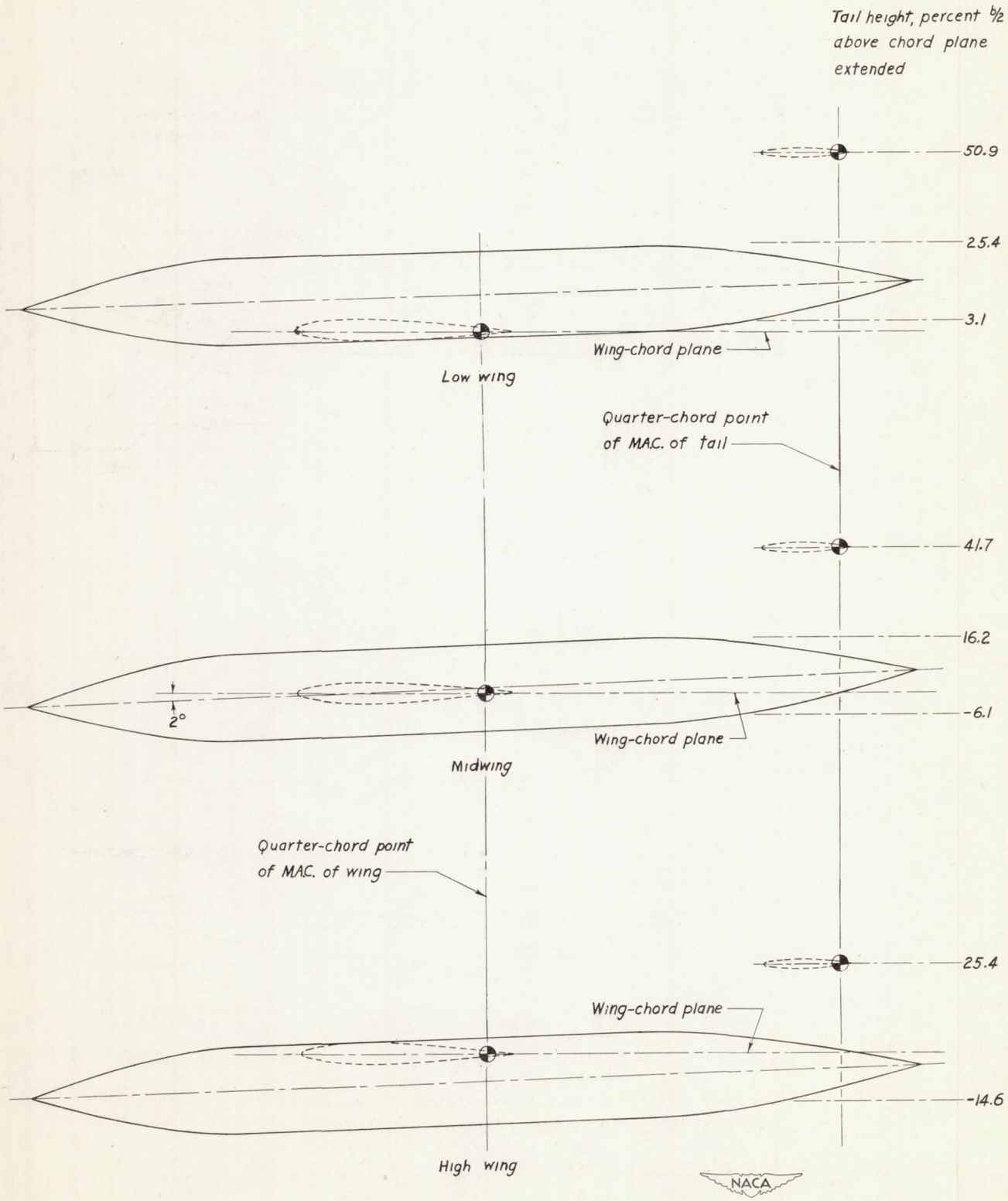

Figure 2.- Vertical location of horizontal tail with respect to wing.

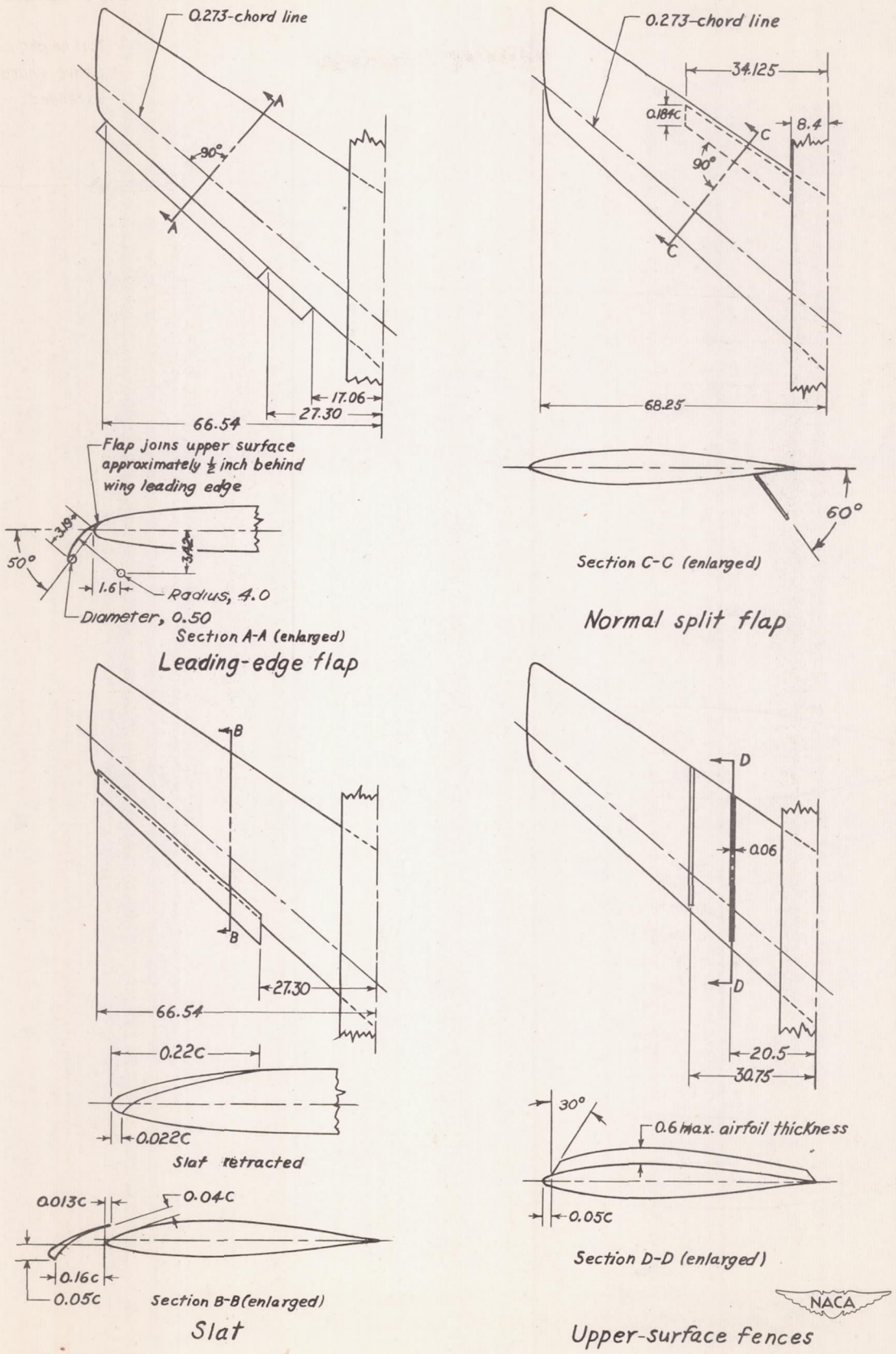

Figure 3.- Details of high-lift and stall-control devices on 42° sweptback wing.

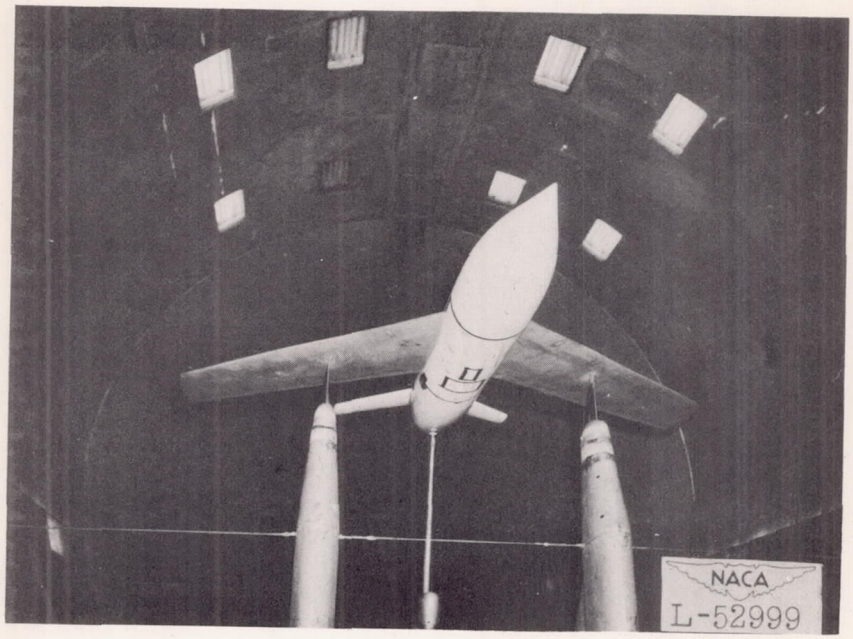

(a) Front view.

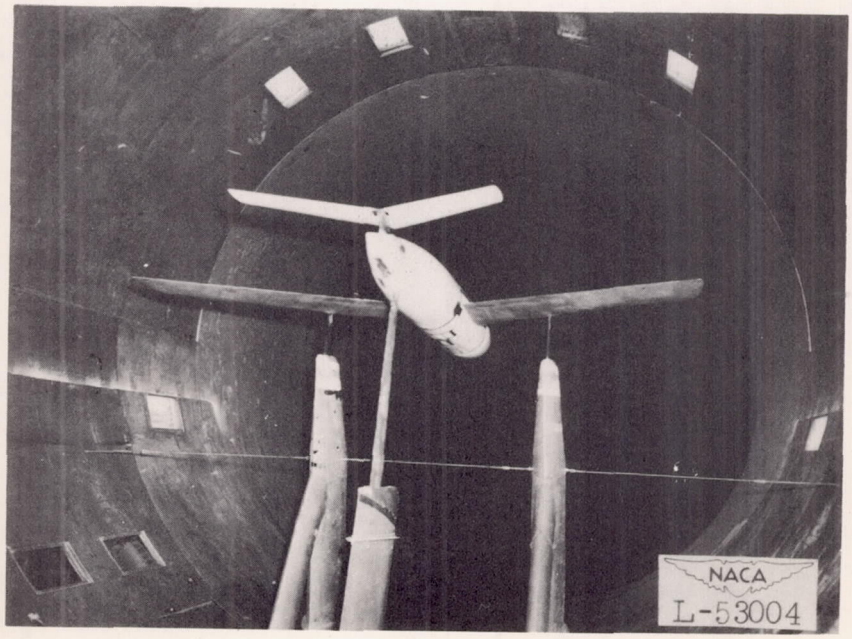

(b) Rear view.

Figure 4.- The 42° sweptback wing-fuselage combination with horizontal tail mounted for testing in the Langley 19-foot pressure tunnel.

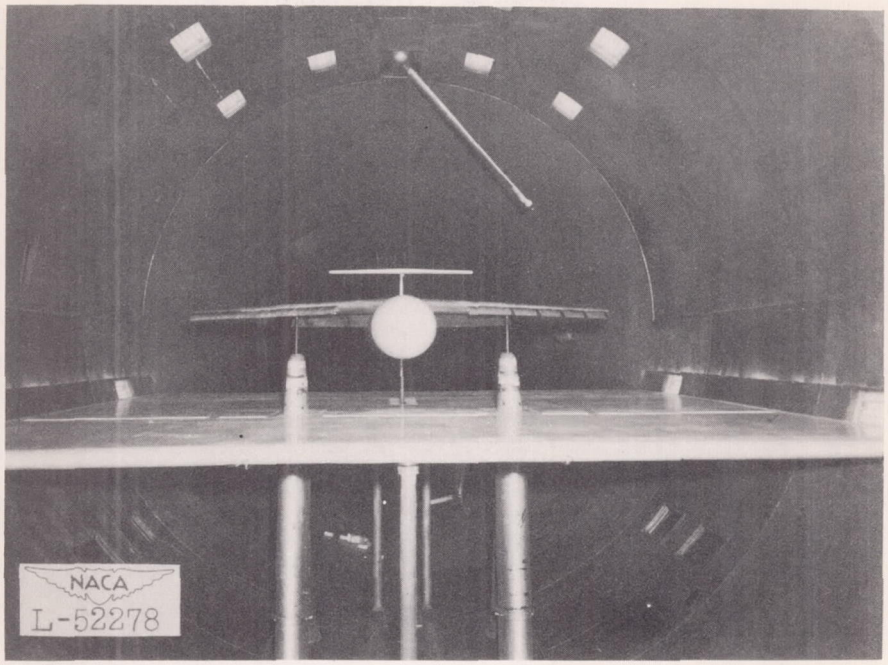

(a) Front view.

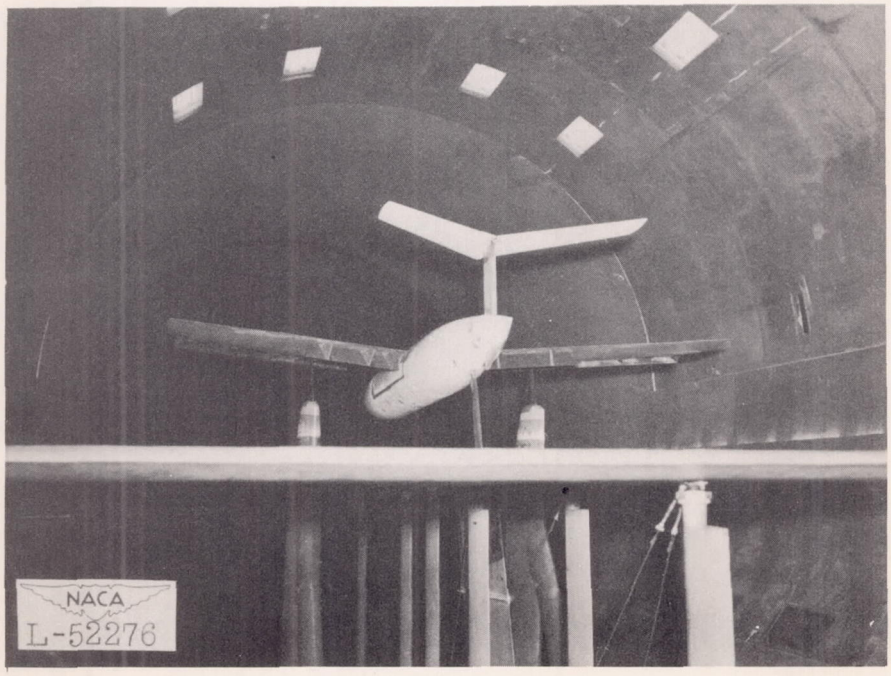

(b) Rear view.

Figure 5.- The 42° sweptback wing-fuselage combination with horizontal tail mounted in the Langley 19-foot pressure tunnel for testing in the presence of a ground board.

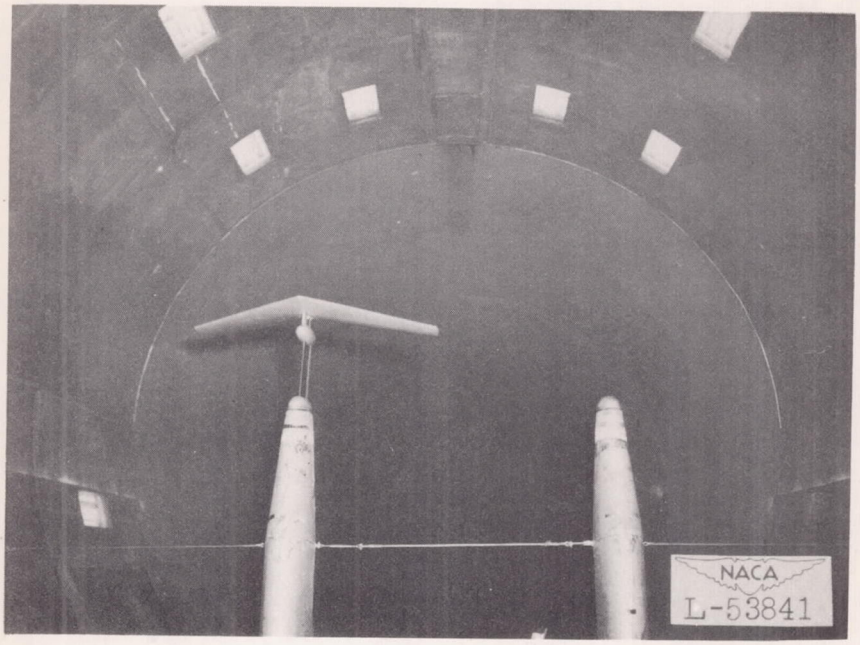

(a) Front view.

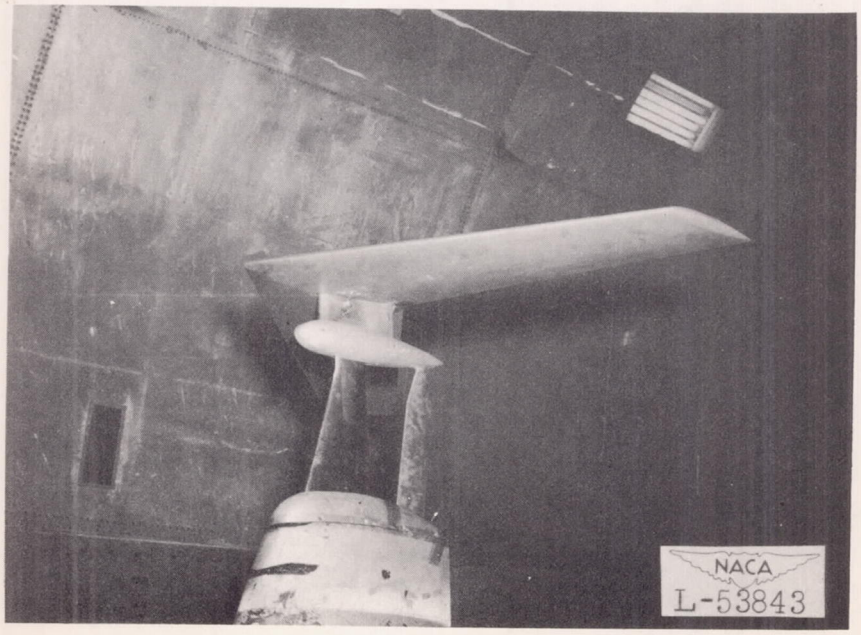

(b) Side view.

Figure 6.- Isolated tail mounted for testing in Langley 19-foot pressure tunnel.

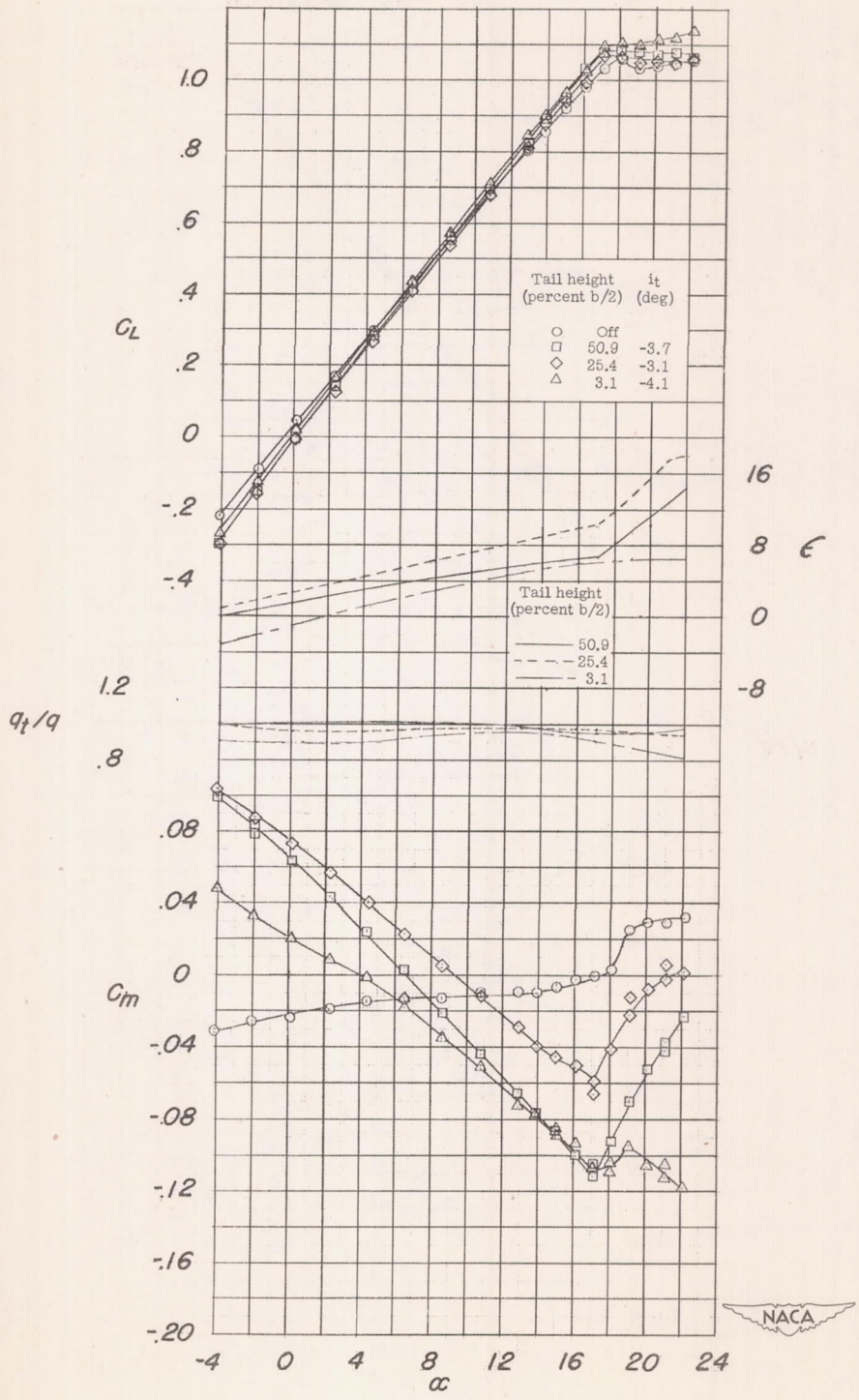

(a) Flaps off; low wing.

Figure 7.- Characteristics of a 42° sweptback wing and fuselage combination.

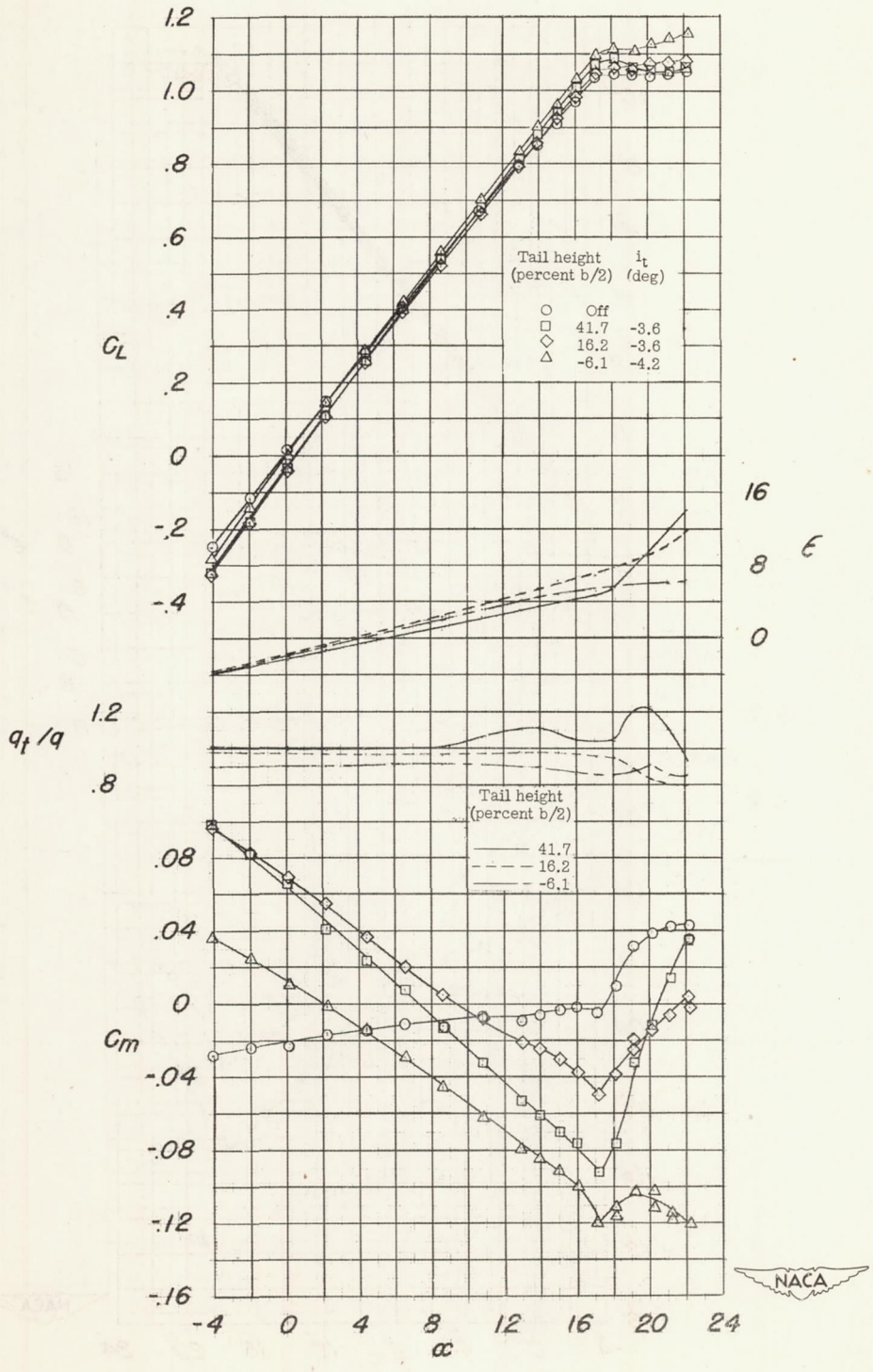

(b) Flaps off; midwing.

Figure 7.- Continued.

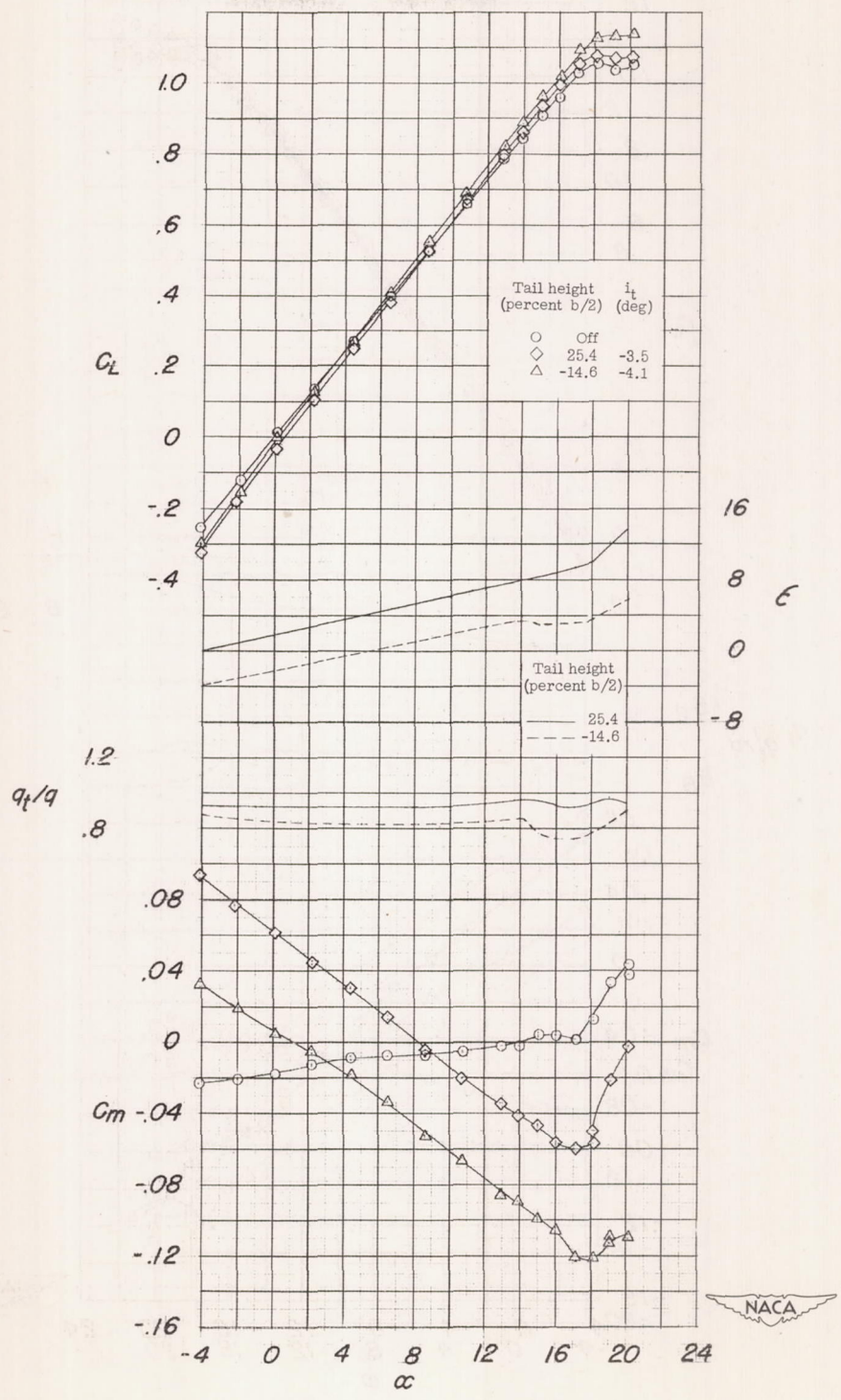

(c) Flaps off; high wing.

Figure 7.- Continued.

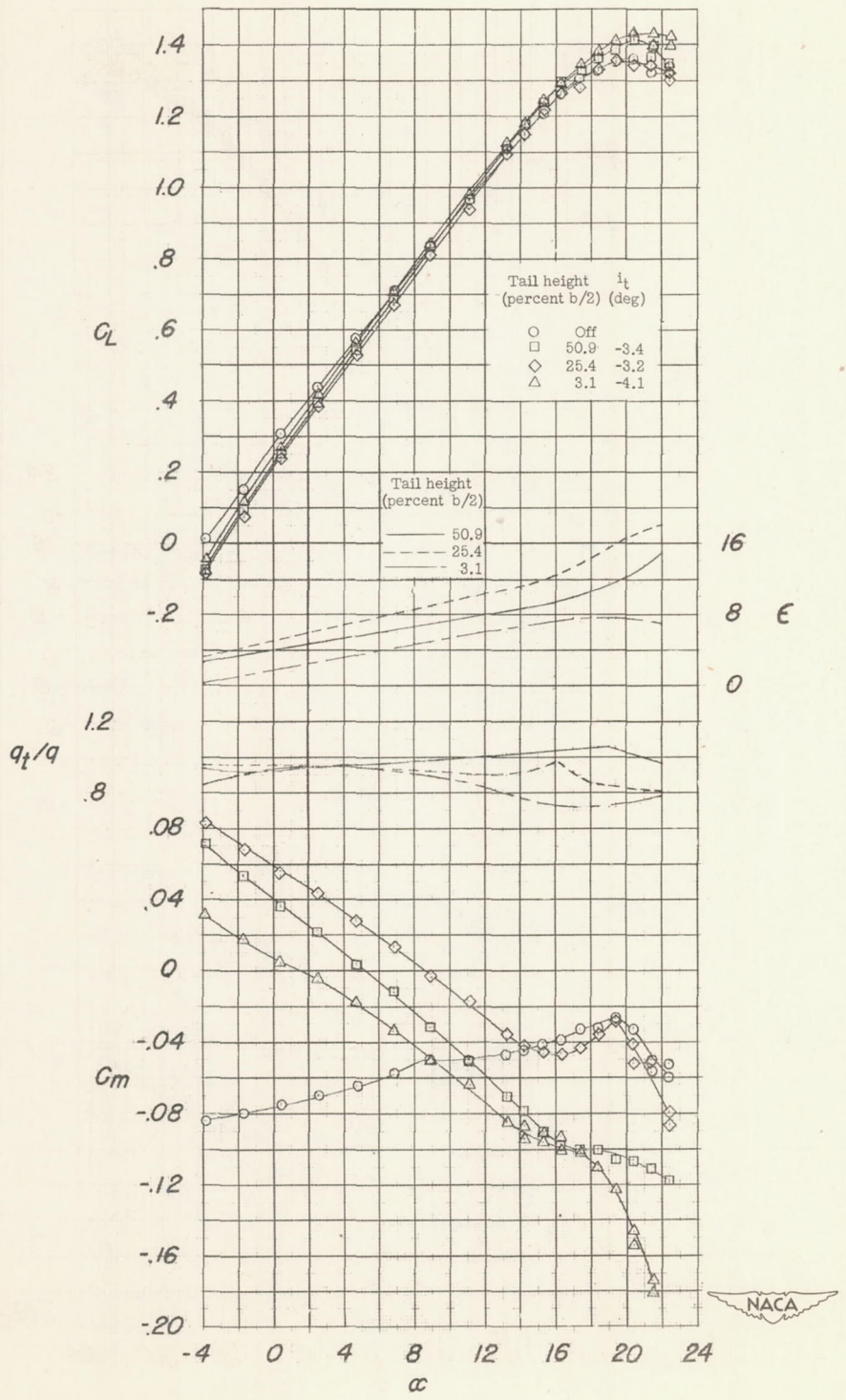

(d) 0.575 $\frac{b}{2}$-span leading-edge flaps; split flaps; low wing.

Figure 7.- Continued.

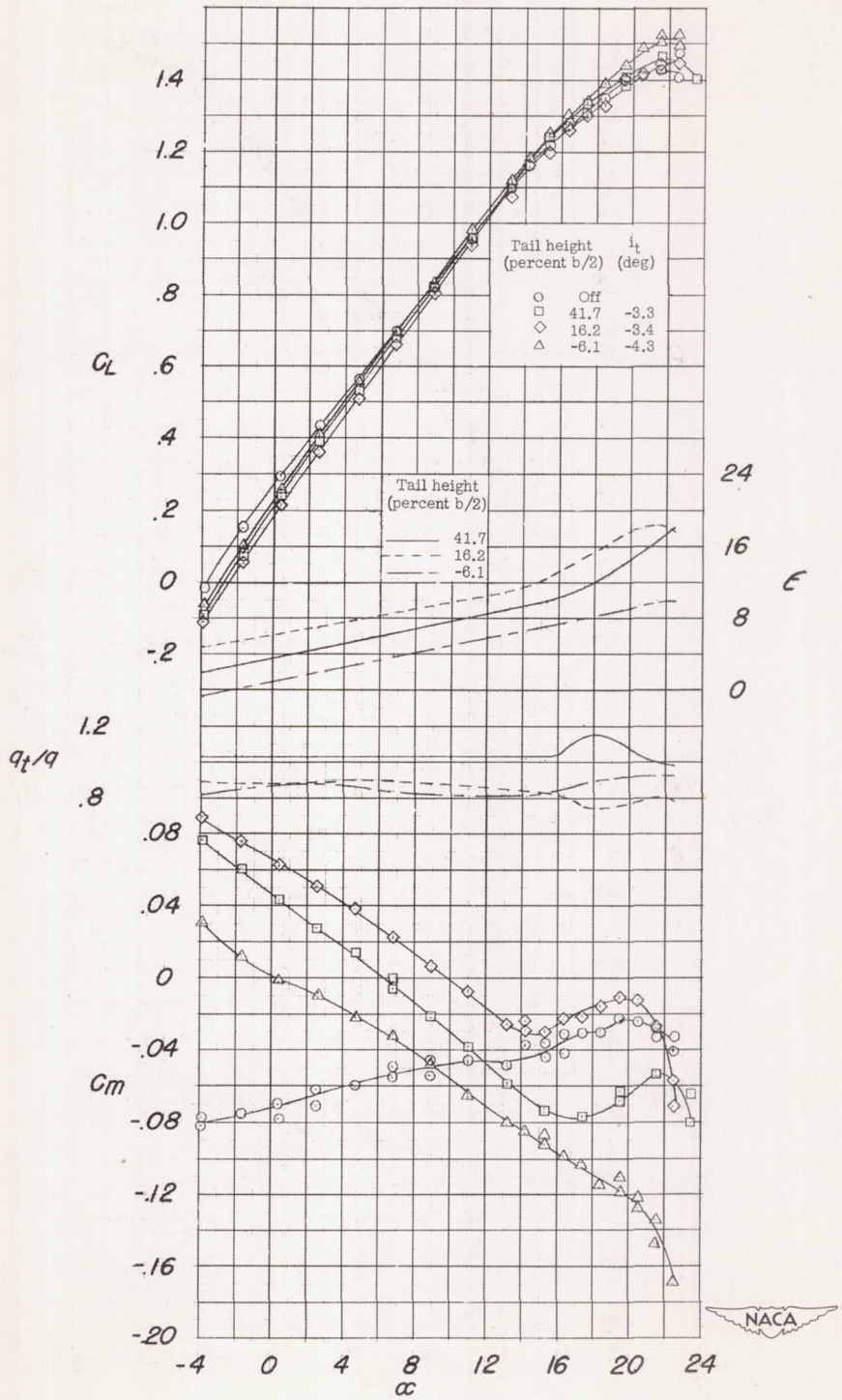

(e) 0.575 $\frac{b}{2}$-span leading-edge flaps; split flaps; midwing.

Figure 7.- Continued.

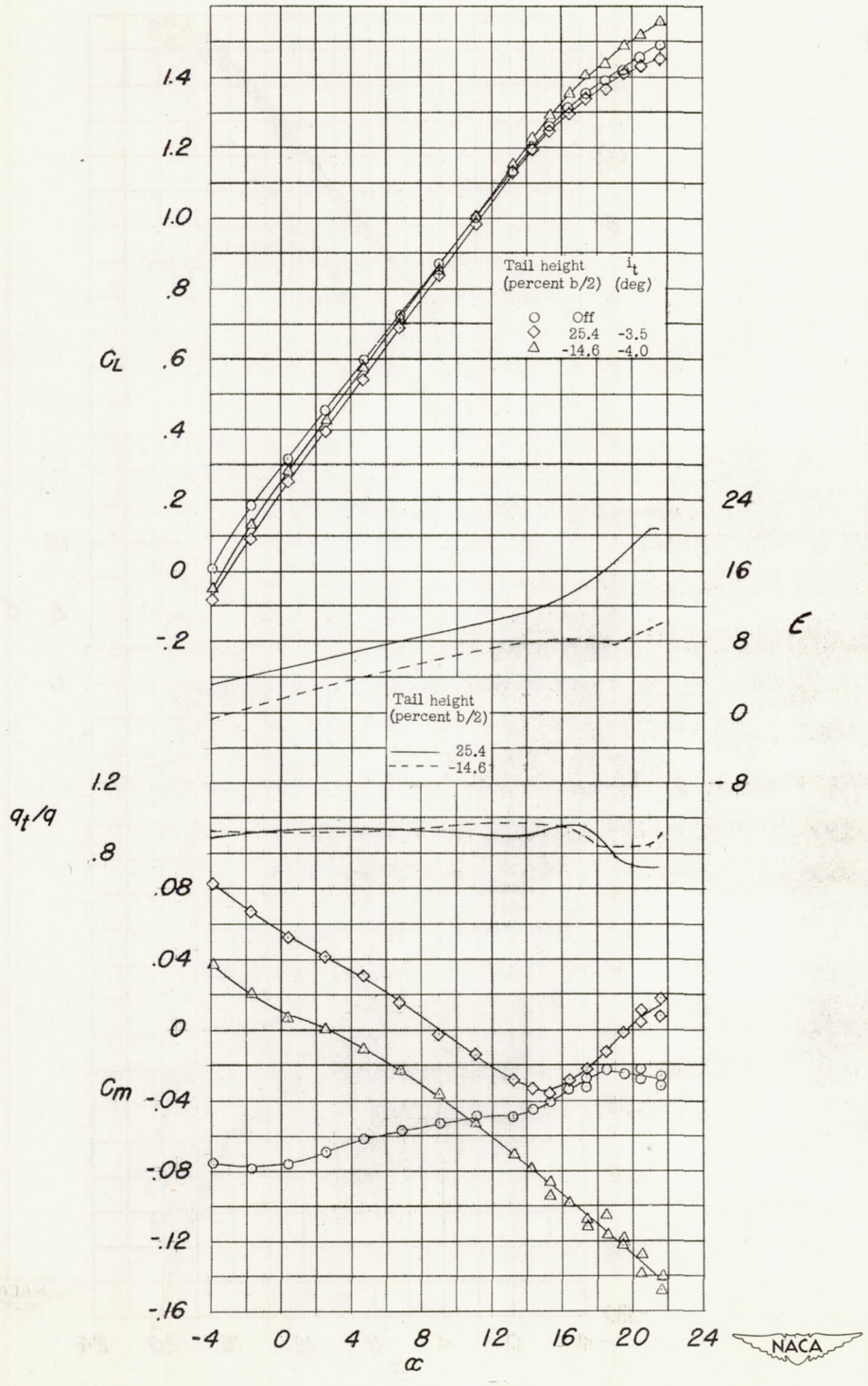

(f) 0.575 $\frac{b}{2}$-span leading-edge flaps; split flaps; high wing.

Figure 7.- Continued.

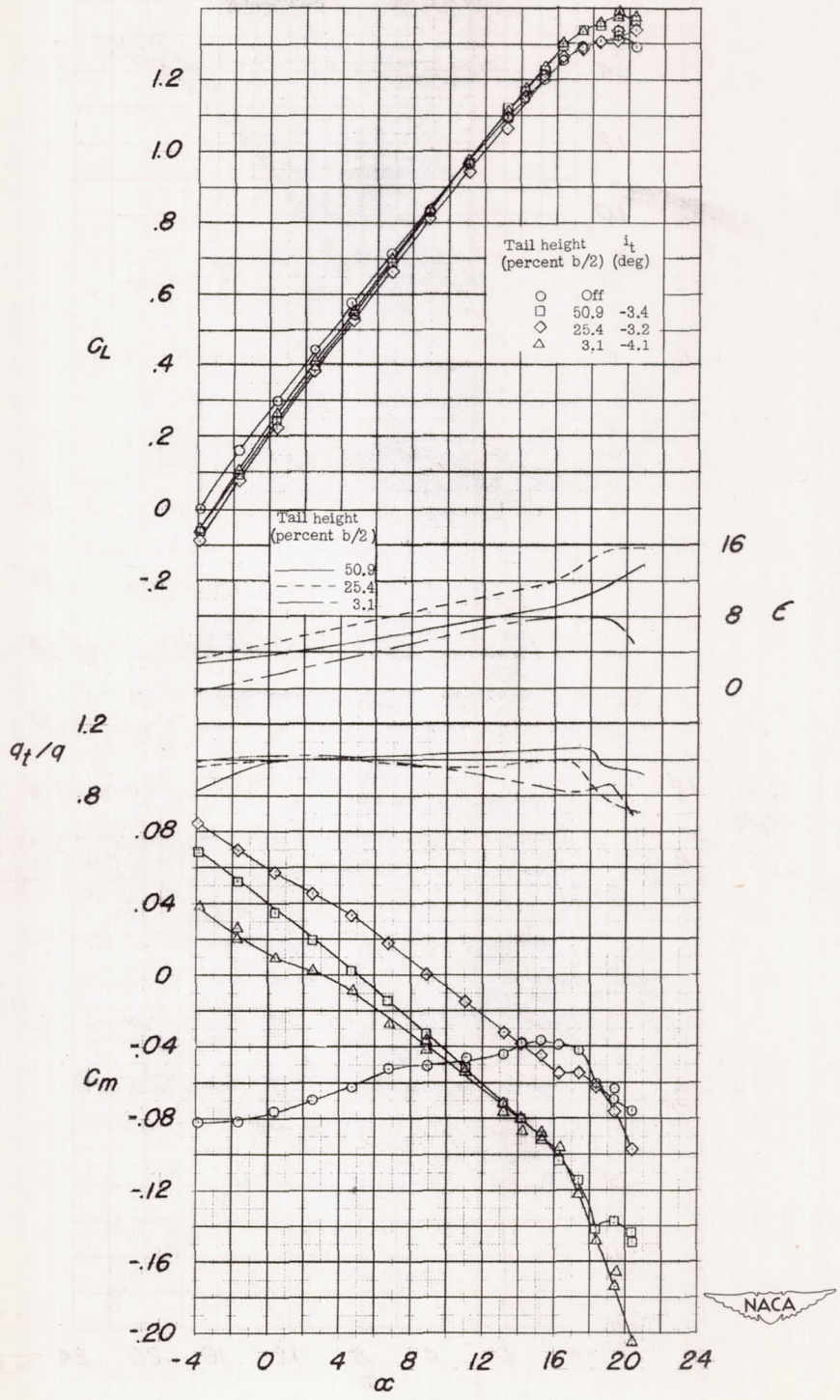

(g) 0.575 $\frac{b}{2}$-span leading-edge flaps; split flaps; upper-surface fences; low wing.

Figure 7.- Continued.

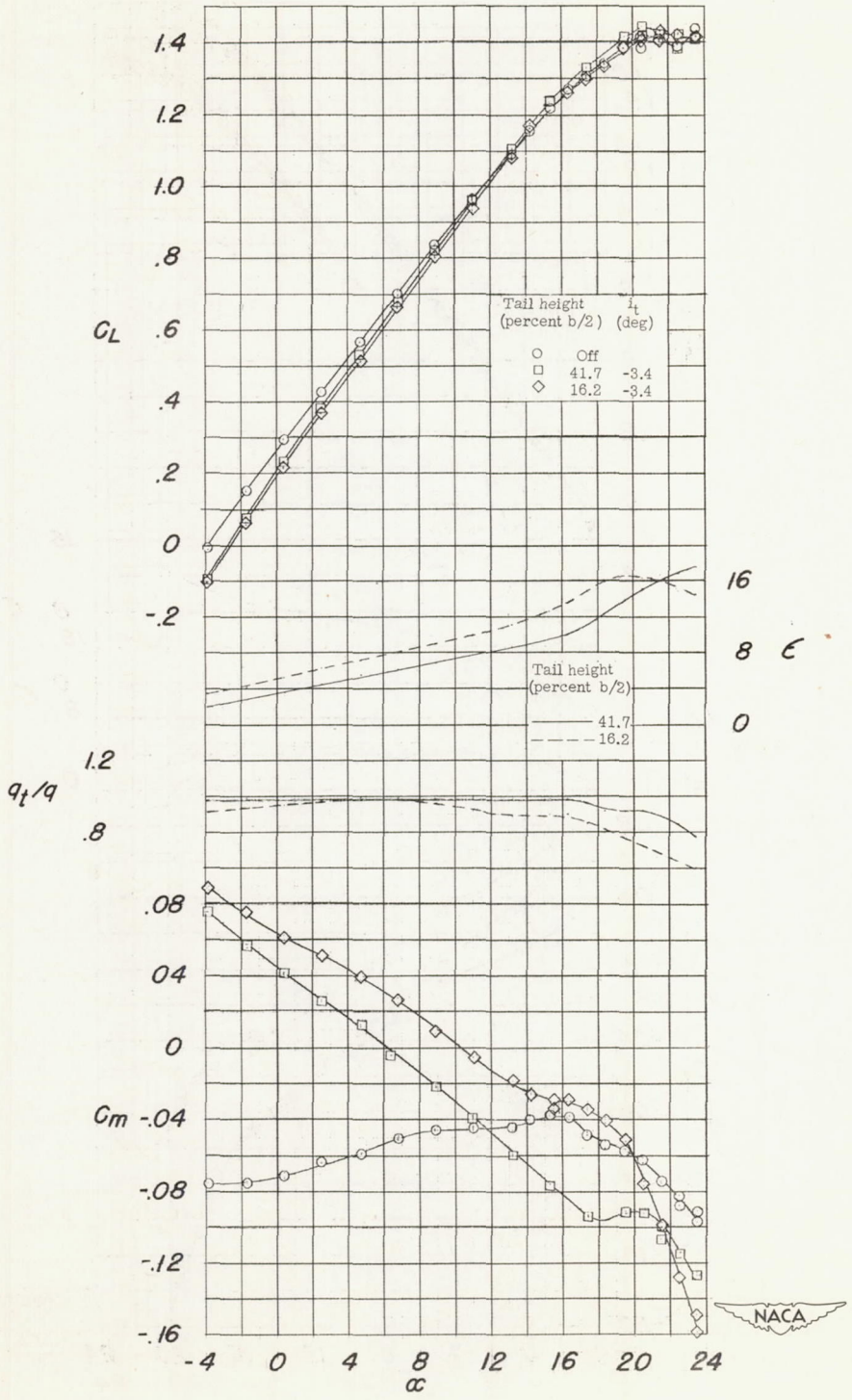

(h) 0.575 $\frac{b}{2}$-span leading-edge flaps; split flaps; upper-surface fences; midwing.

Figure 7.- Continued.

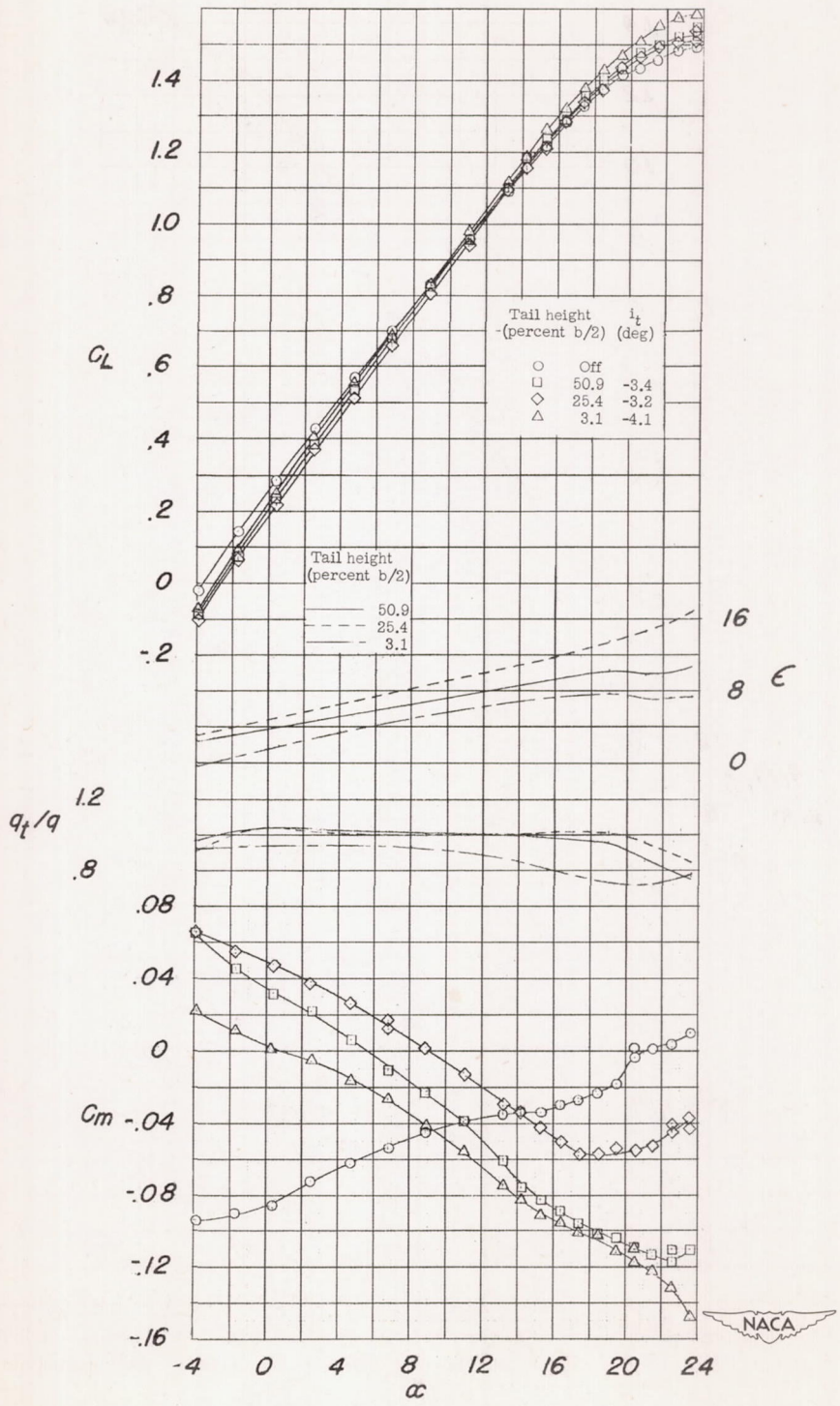

(i) 0.725 $\frac{b}{2}$-span leading-edge flaps; split flaps; low wing.

Figure 7.- Continued.

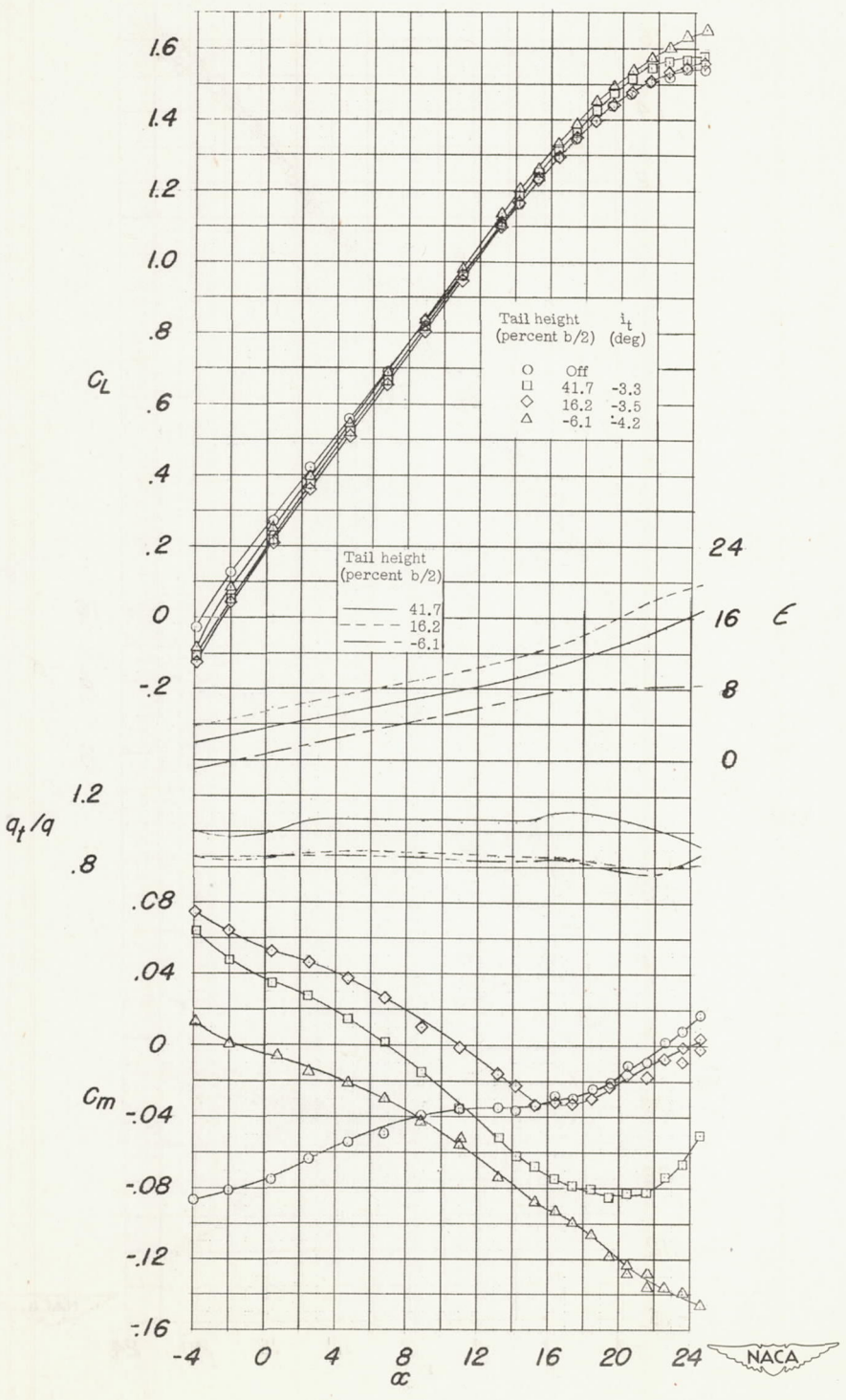

(j) 0.725 $\frac{b}{2}$-span leading-edge flaps; split flaps; midwing.

Figure 7.- Continued.

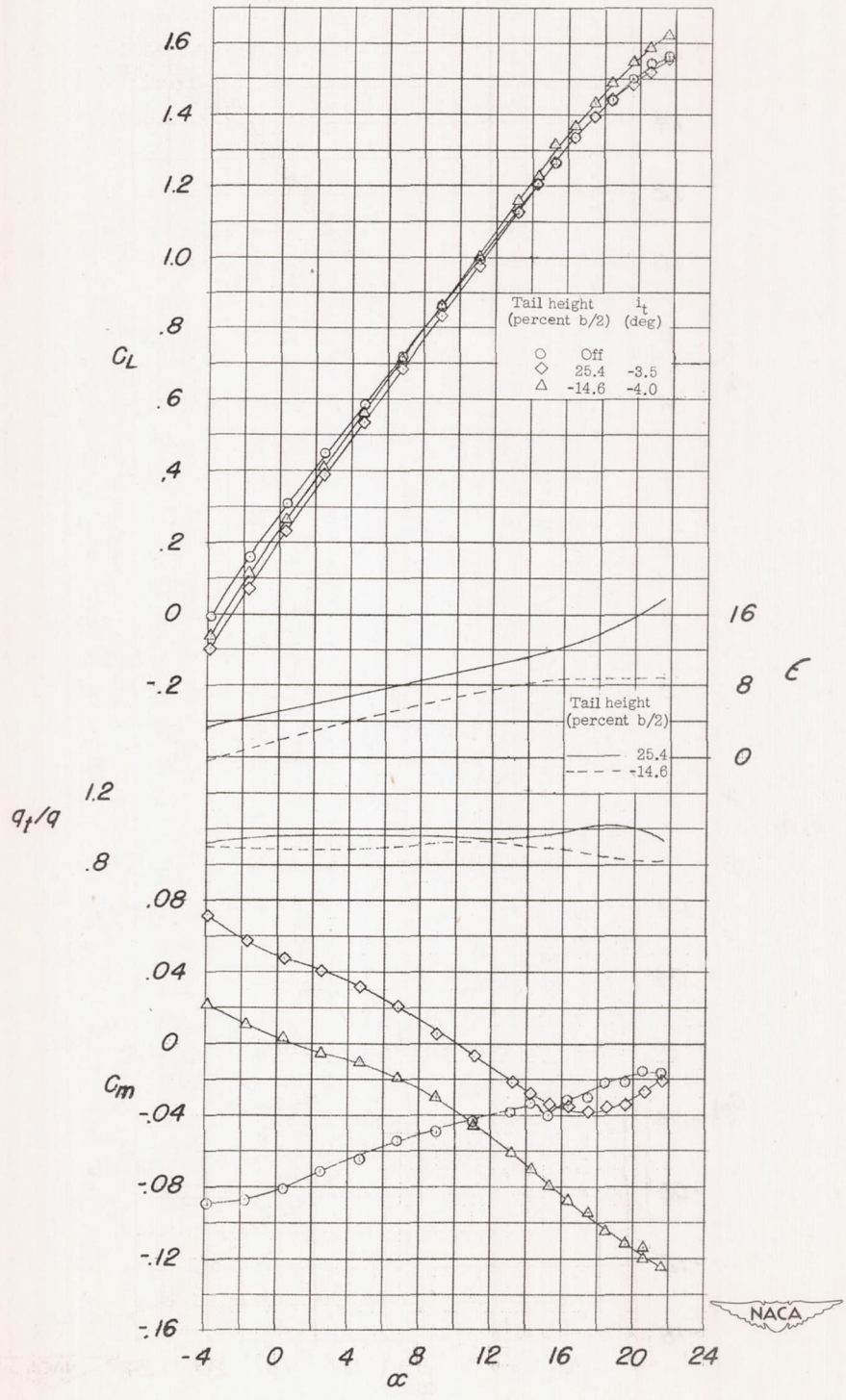

(k) 0.725 $\frac{b}{2}$-span leading-edge flaps; split flaps; high wing.

Figure 7.- Continued.

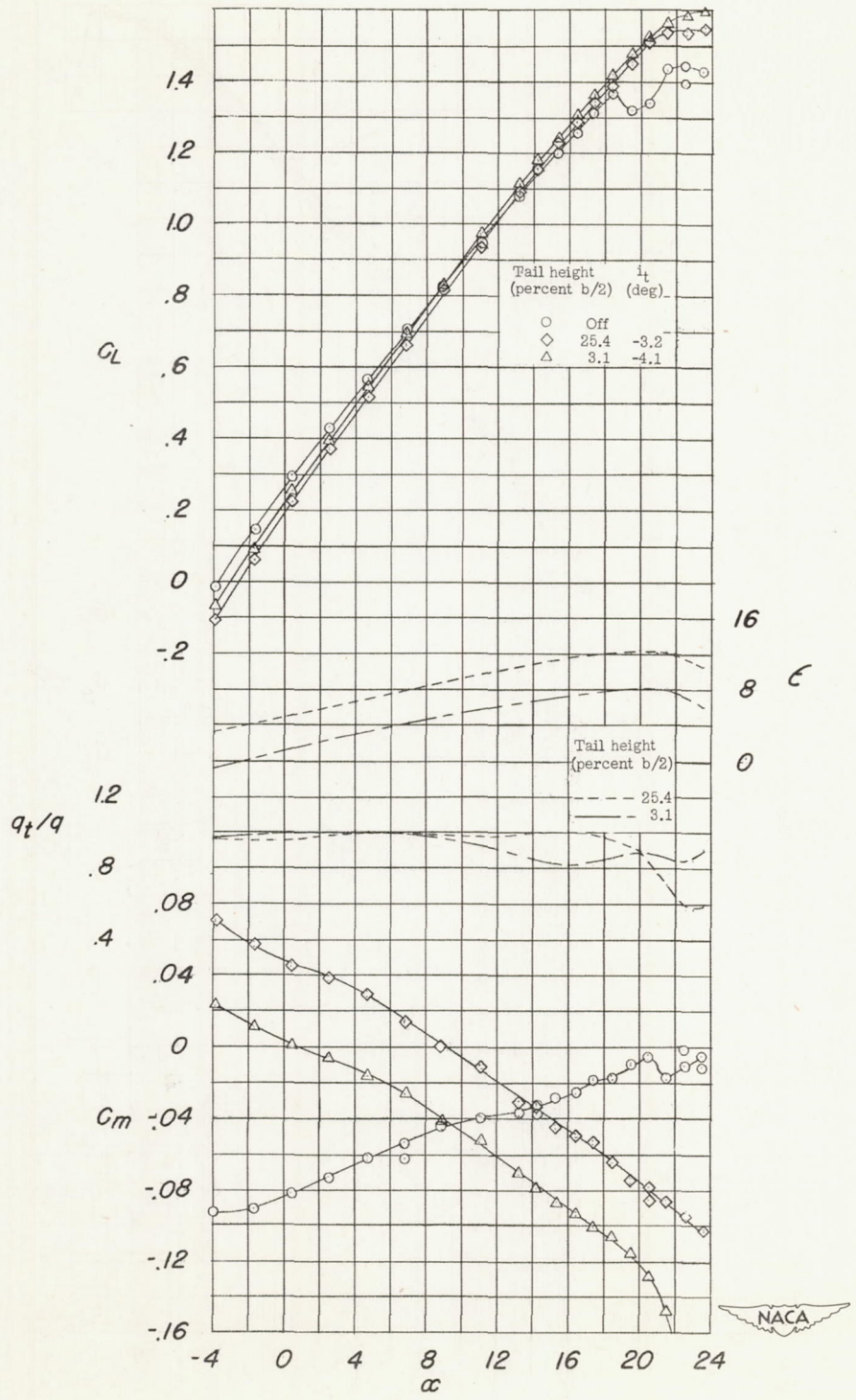

(l) 0.725 $\frac{b}{2}$ -span leading-edge flaps; split flaps; upper-surface fences; low wing.

Figure 7.- Continued.

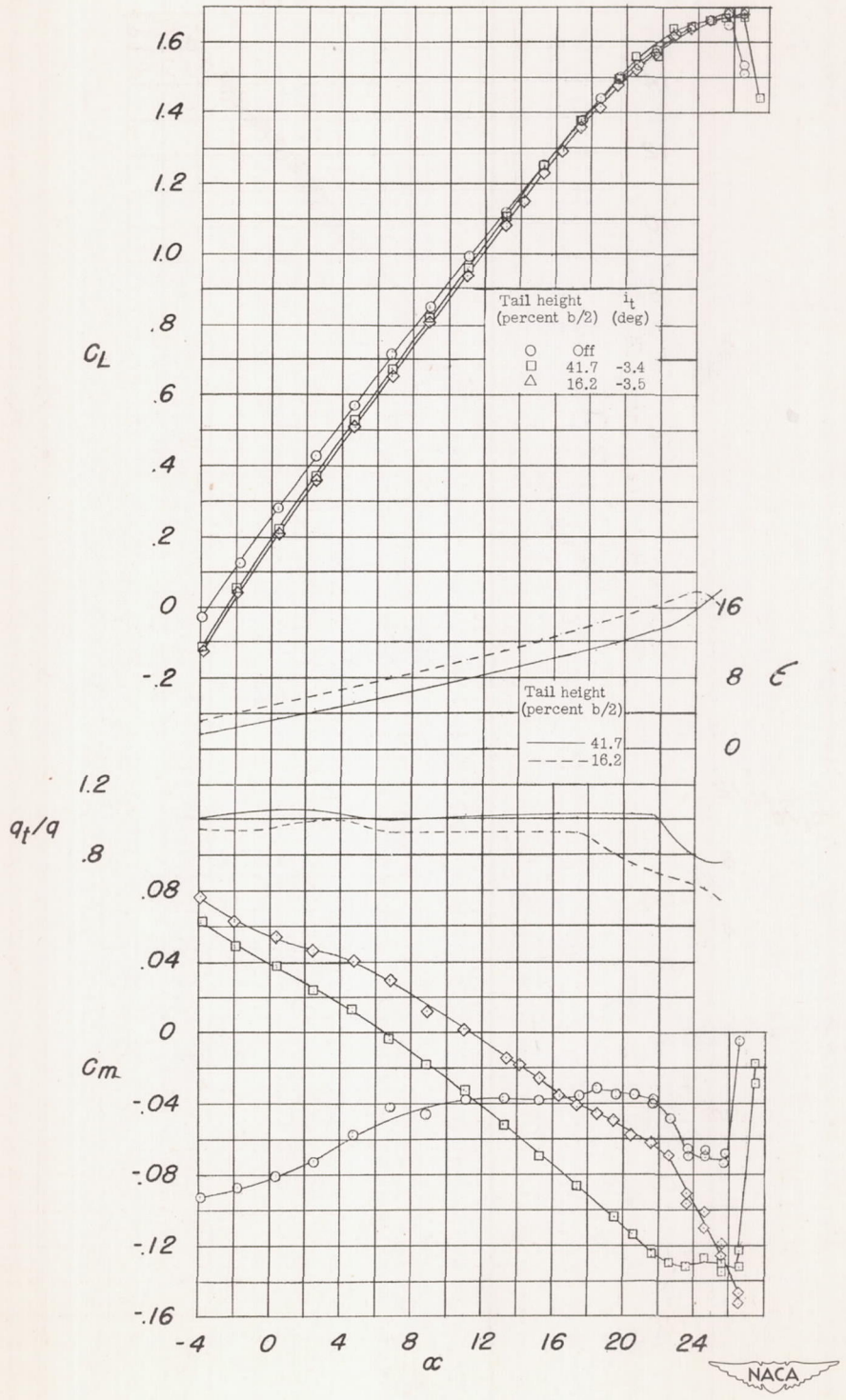

(m) 0.725 $\frac{b}{2}$-span leading-edge flaps; split flaps; upper-surface fences; midwing.

Figure 7.- Continued.

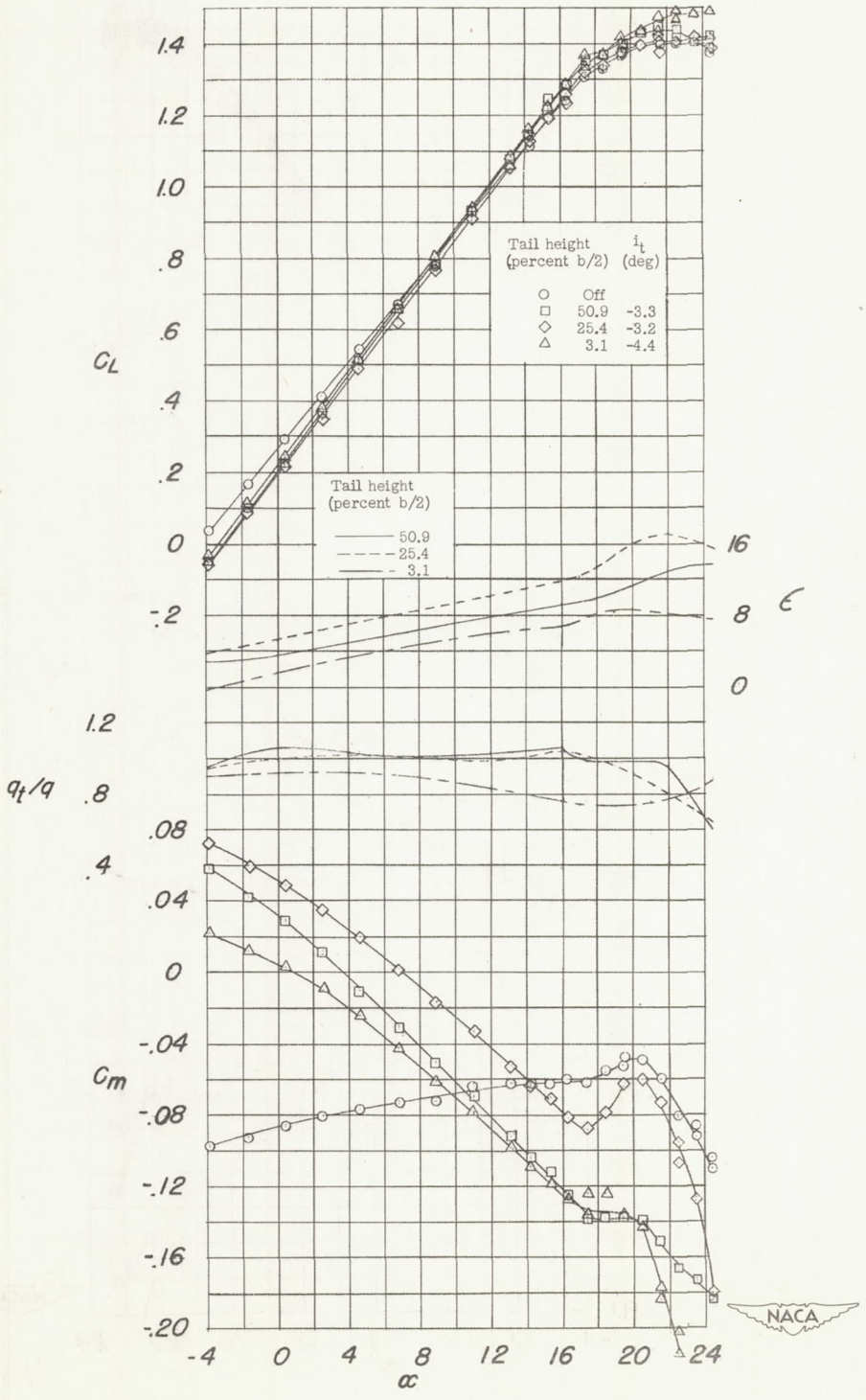

(n) 0.575 $\frac{b}{2}$-span slat; split flaps; low wing.

Figure 7.- Continued.

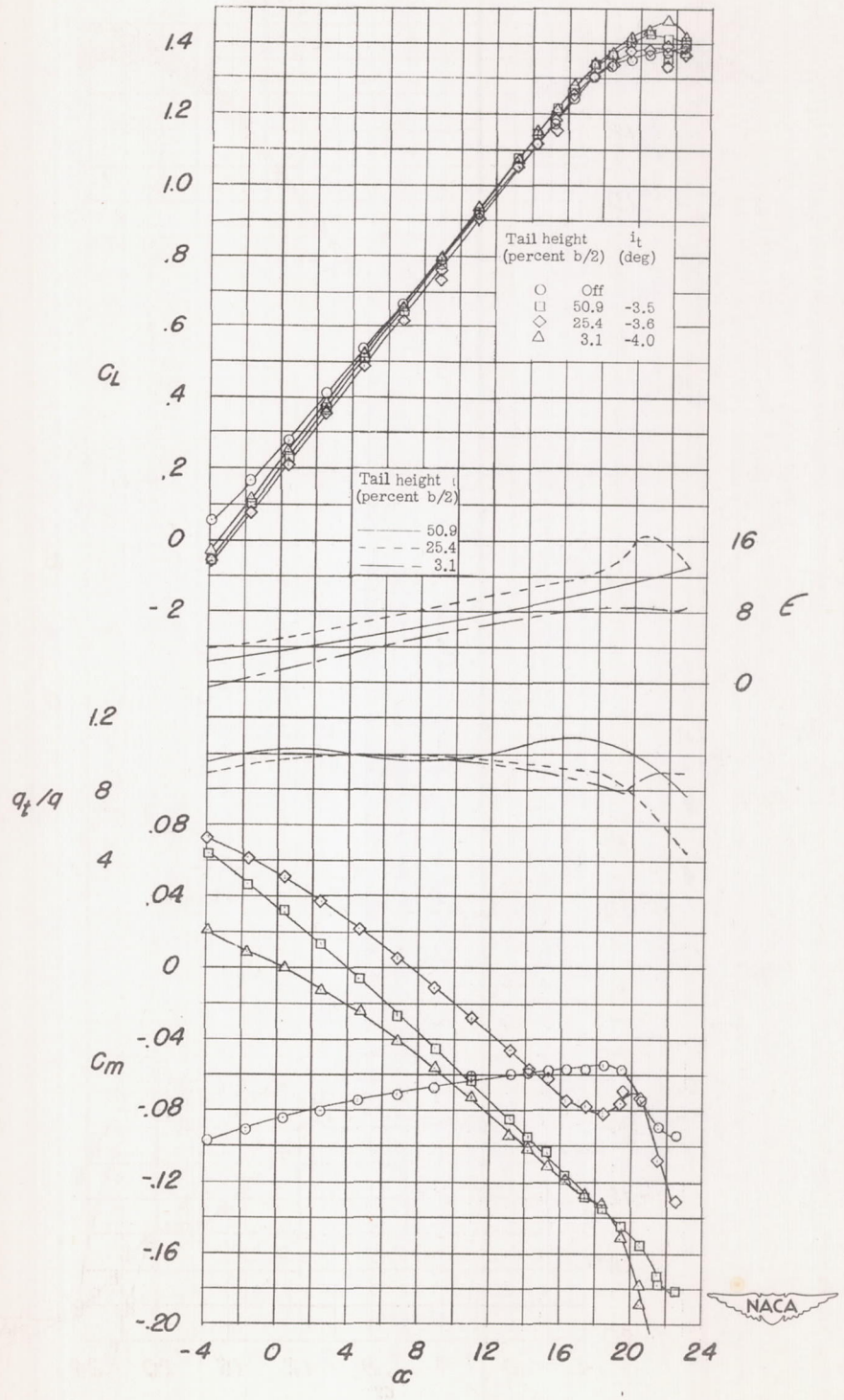

(o) 0.575 $\frac{b}{2}$-span slat; split flaps; upper-surface fences; low wing.

Figure 7.- Continued.

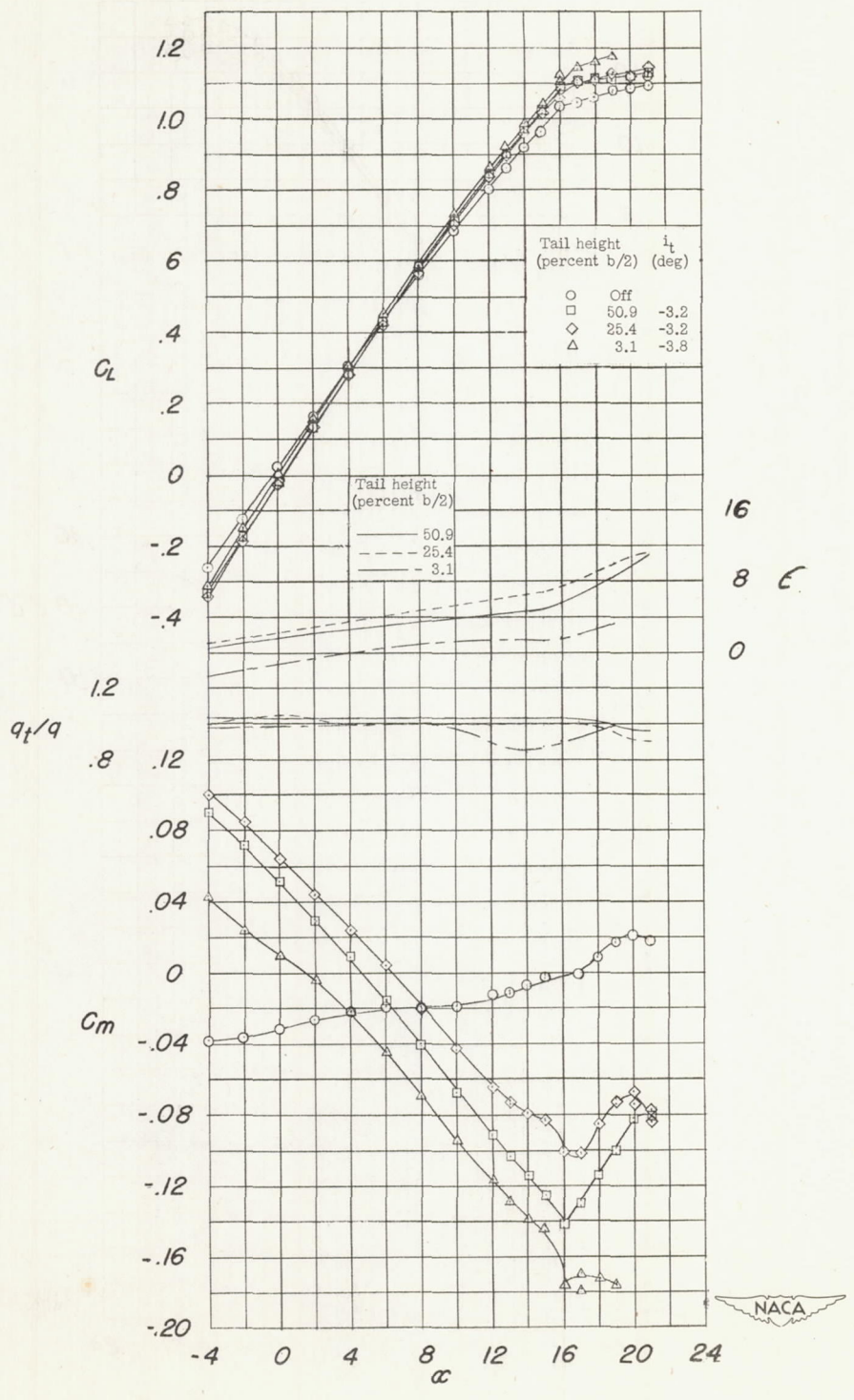

(p) Flaps off; low wing; ground board in.

Figure 7.- Continued.

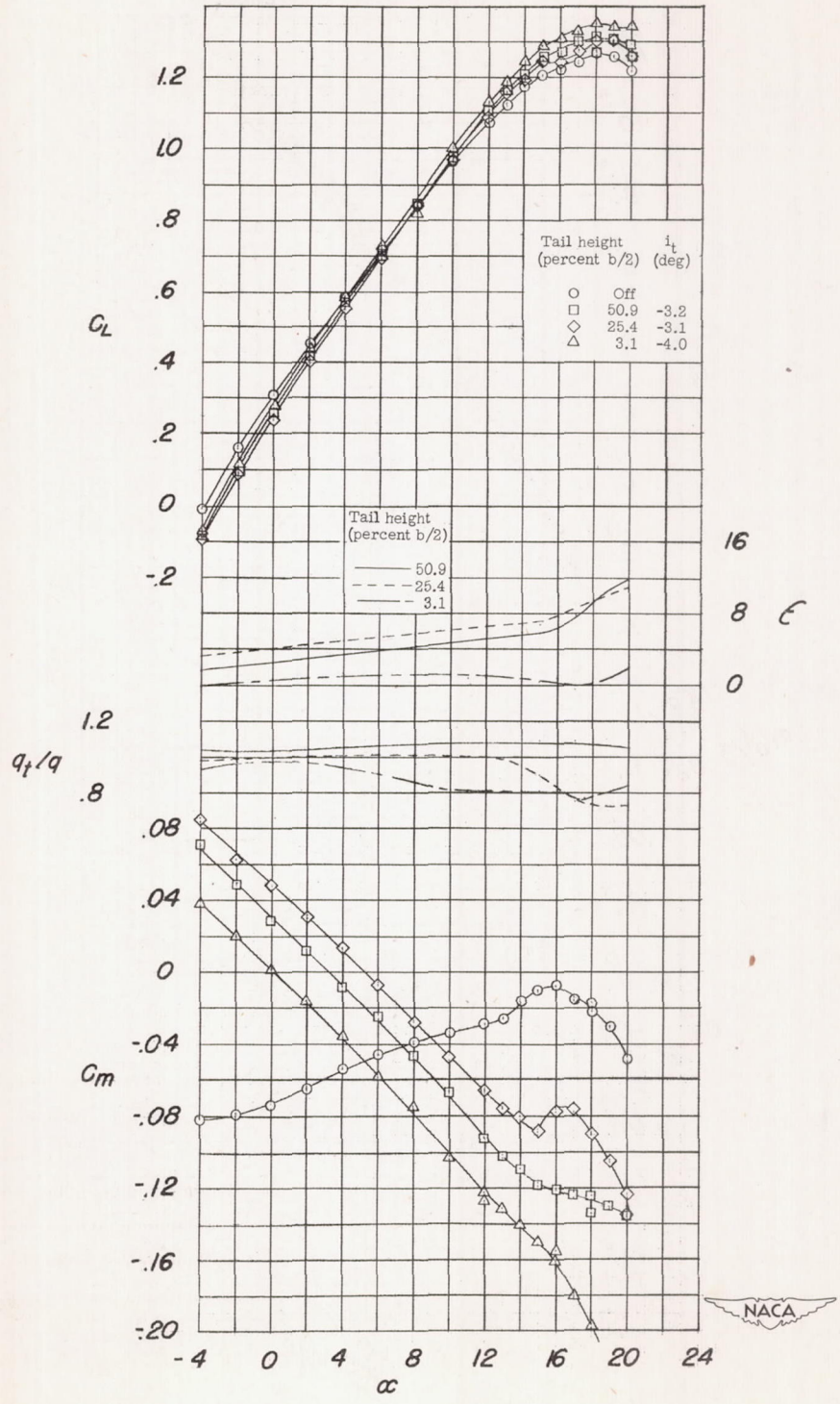

(q) 0.575 $\frac{b}{2}$-span leading-edge flaps; split flaps; low wing; ground board in.

Figure 7.- Continued.

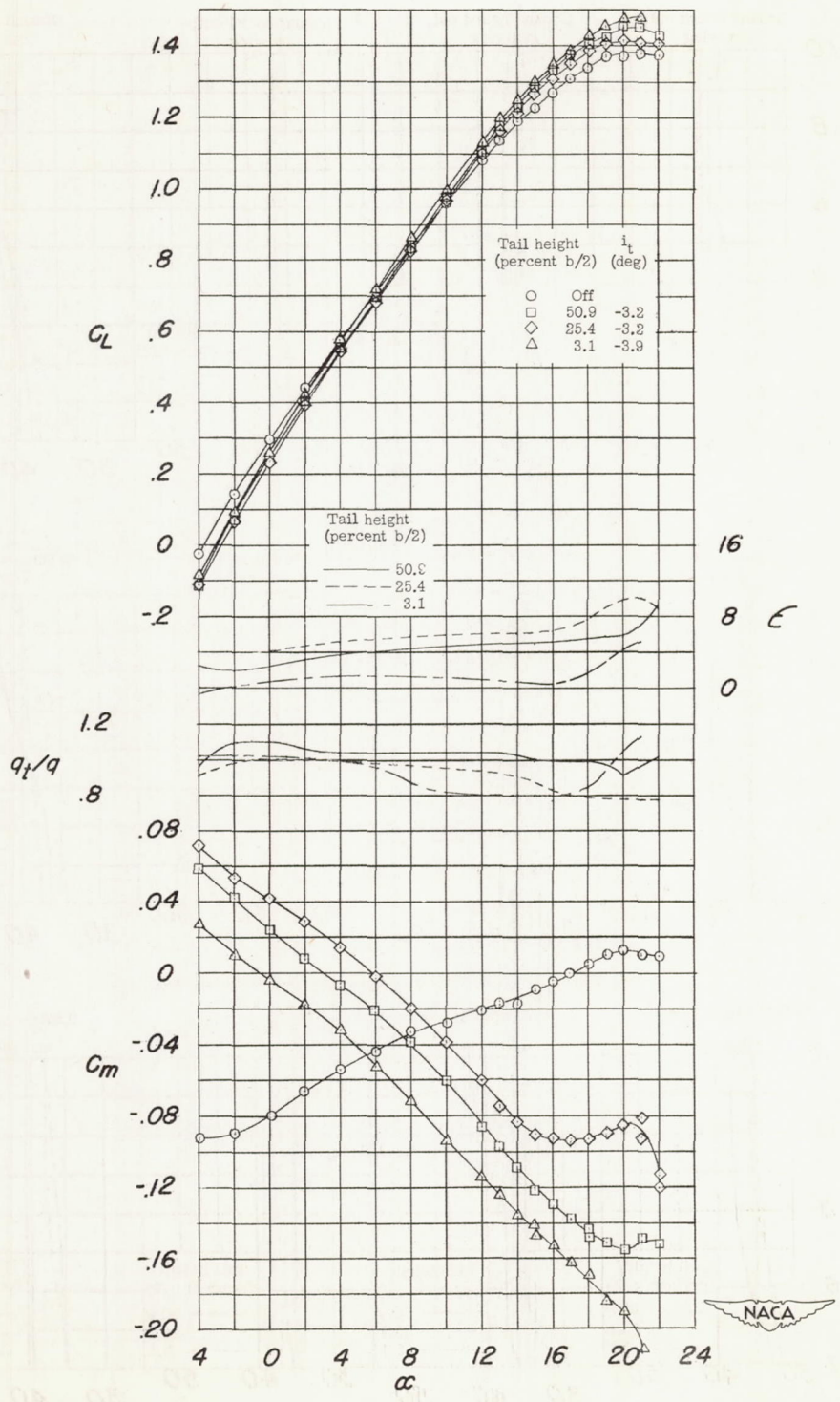

(r) 0.725 $\frac{b}{2}$-span leading-edge flaps; split flaps; low wing; ground board in.

Figure 7.- Concluded.

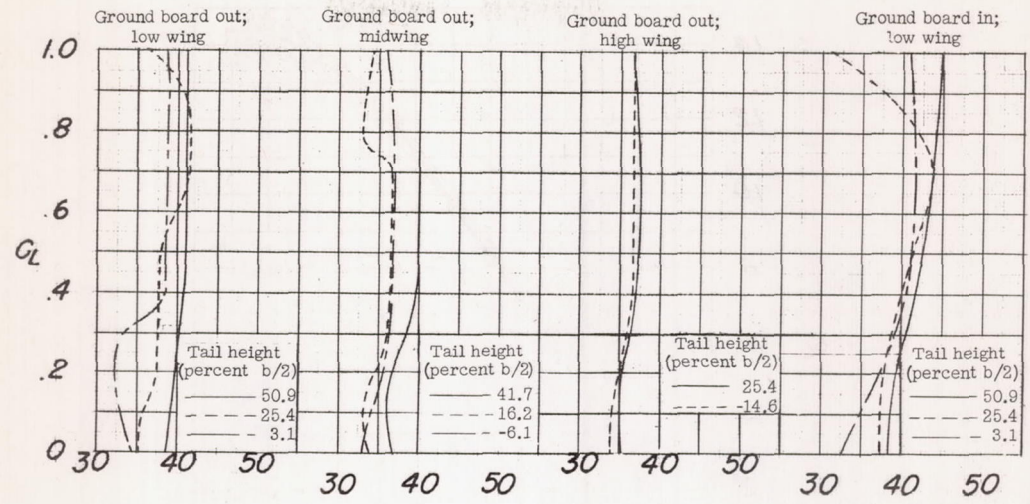

(a) Wing without flaps.

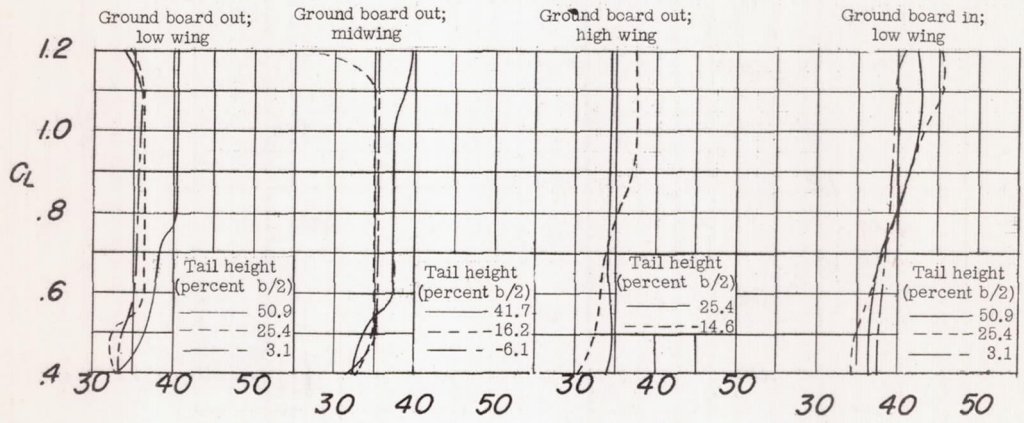

(b) Wing with $0.575\frac{b}{2}$-span leading-edge flap and split flap.

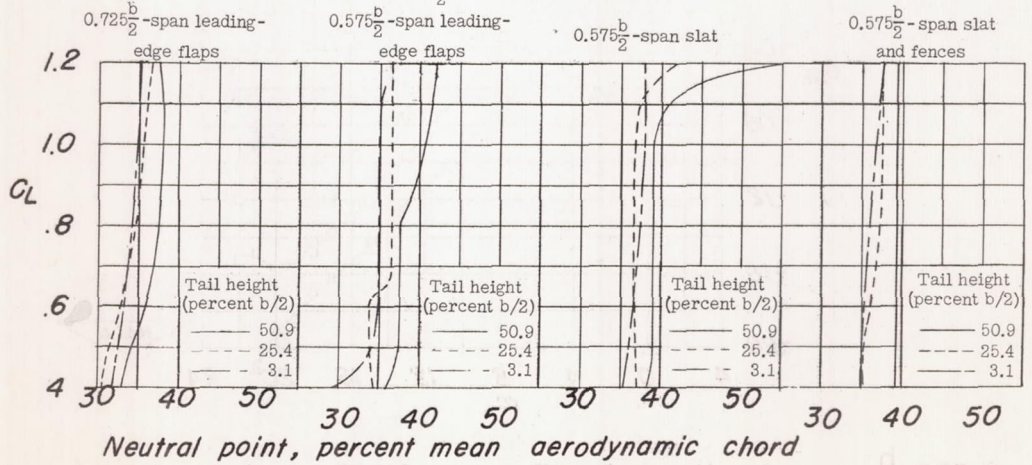

(c) Low wing position; ground board out.

Figure 8.- Neutral-point characteristics of 42° sweptback wing-fuselage combination.

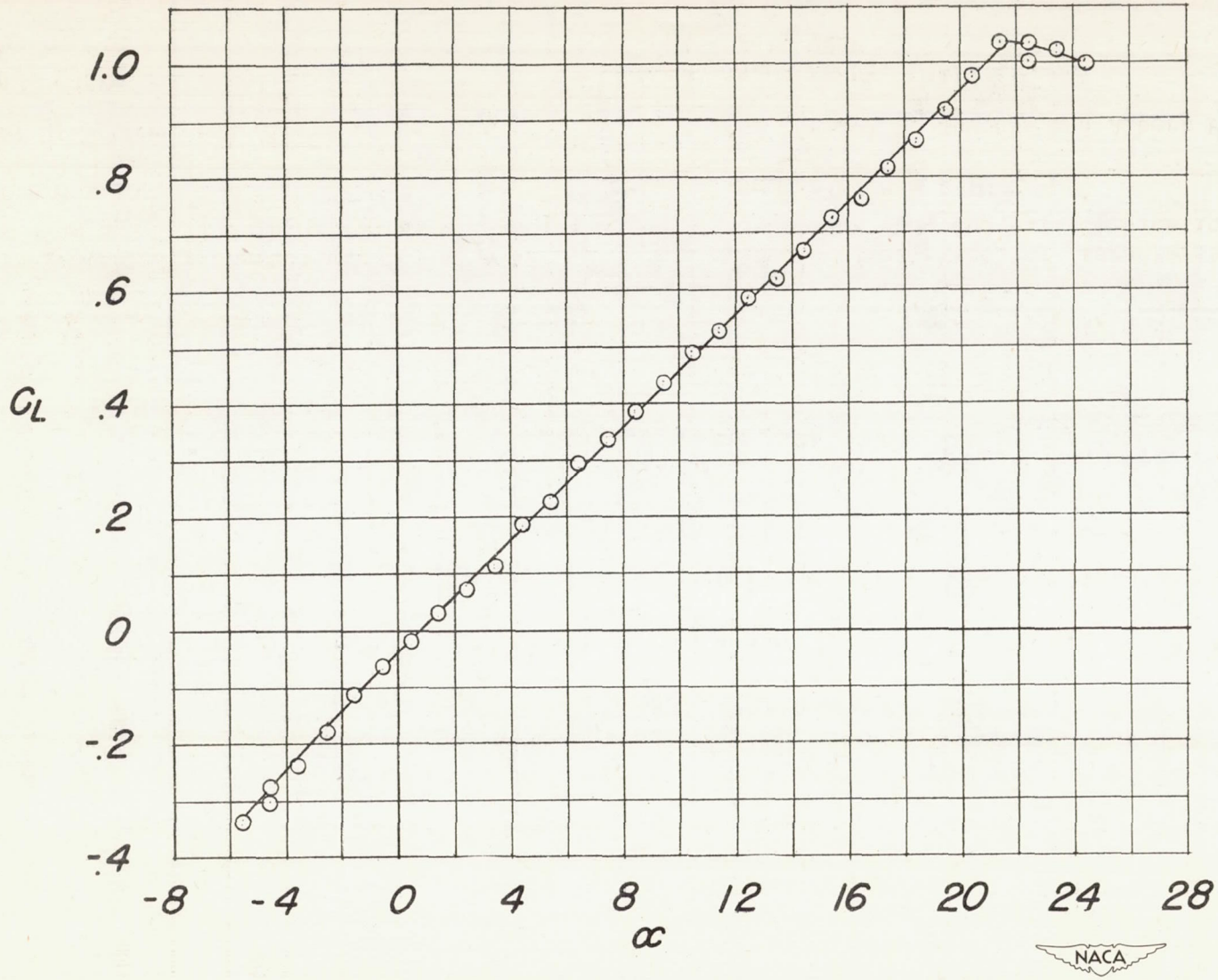

Figure 9.- Lift characteristics of isolated tail.